Journal of Archaeological Science 135 (2021) 105489

Contents lists available at ScienceDirect

Journal of Archaeological Science

journal homepage: www.elsevier.com/locate/jas

Modelling a scale-based strontium isotope baseline for Hungary

Margaux L.C. Depaermentier [a,**,1], Michael Kempf [b,c,*,1], Eszter Bánffy [d], Kurt W. Alt [e,f]

[a] Department of Early Medieval and Roman Provincial Archaeology, University of Basel, Basel, Switzerland
[b] Department of Archaeology and Museology, Faculty of Arts, Masaryk University, Brno, Czech Republic
[c] Institute of Environmental Social Science and Geography, University of Freiburg, Freiburg, Germany
[d] Romano-Germanic Commission of the German Archaeological Institute, Frankfurt/Main, Germany
[e] Center of Natural and Cultural Human History, Danube Private University, Krems-Stein, Austria
[f] Department of Integrative Prehistory and Archaeological Science, University of Basel, Basel, Switzerland

ARTICLE INFO

Keywords:
Carpathian basin
Strontium isotope analysis
Environmental modelling
Micro-regional scale
Site-specific scale

ABSTRACT

Strontium isotope analysis has recently proven to be a useful tool to elucidate population movements and subsistence strategies in ecological and archaeological sciences. The interpretation depends on the size, type, availability, and preservation of the sample and the reliability of the produced strontium isotope baseline. However, collecting quantitatively and qualitatively suitable baseline samples is considered a challenging task in archaeological research. To meet these challenges, we introduce an innovative analytical technique, which enables the analysis of small sample sizes from heterogeneous site distribution and environmental settings. This article integrates multivariate environmental modelling and bioarchaeological data of 49 sites to establish the first scale-based differentiation between site-specific and micro-regional strontium isotope baselines with various sample sizes in Hungary. In future mobility studies, this approach will allow distinguishing human and faunal movement ranges on different geographical scales.

1. Introduction

Strontium isotope analyses have proven their potential in archaeological research that aimed to reconstruct mobility patterns (Alt et al., 2014; Depaermentier et al., 2020a; Knipper et al., 2020; Whittle et al., 2013), husbandry strategies (Balasse et al., 2002; Gerling et al., 2012, 2017), and socio-cultural structures (Knipper, 2017; Knipper et al., 2020) within past societies. However, the analyses require the determination of local isotope baselines, whose reliability is closely linked to the size, type, availability, and preservation of the baseline sample (Gerling, 2015; Makarewicz and Sealy, 2015). Because the bioavailable strontium composition depends mostly on the geological and pedological settings, soil samples and published $^{87}Sr/^{86}Sr$ ratios of the geological units are widely used to determine a local strontium isotope baseline (Brönnimann et al., 2018; Giblin, 2009; Heinrich-Tamáska and Schweissing, 2011; Knudson et al., 2014; Shaw et al., 2009; Whittle et al., 2013). However, other environmental parameters such as sea-spray-effect in coastal areas can impact the local strontium composition, rendering reliance on only geological data unreliable (Alonzi et al., 2020; Bentley, 2006; Makarewicz and Sealy, 2015; Montgomery, 2010; Naumann et al., 2014; Price et al., 2002; Wong et al., 2018). The abundance and distribution of various rock minerals are further important factors that complicate obtaining representative data from soil samples due to weathering processes (Bentley, 2006).

This also applies for water samples, which can show $^{87}Sr/^{86}Sr$ ratios that correspond to the mixed signal of different geological and sedimentological units, particularly in large hydrologic systems like the river Tisza and the Danube floodplains. Furthermore, the strontium isotope composition of water is inherently diluted and has only small influence on the isotope composition of human tissues. Because plants absorb the biologically available strontium and their strontium isotope composition is crucial for the isotope abundance within the human tissues, they could be considered a substantially more suitable sample category (Corti et al., 2013; Knipper, 2004; Wong et al., 2018). However, the samples should be taken in considerable distance from modern arable fields or in forested areas to avoid contamination by modern fertilizers (Alt et al., 2014; Brönnimann et al., 2018).

Recent research used comparison data from substrate samples to

* Corresponding author. Institute of Archaeology and Museology, Faculty of Arts, Masaryk University, Arne Nováka 1, Brno, 60200, Czech Republic.
** Corresponding author. Department of Early Medieval and Roman Provincial Archaeology, University of Basel, Petersgraben 51, 4051, Basel, Switzerland.
E-mail addresses: m.depaermentier@unibas.ch (M.L.C. Depaermentier), kempf@phil.muni.cz (M. Kempf).
[1] These authors contributed equally to this work.

https://doi.org/10.1016/j.jas.2021.105489
Received 29 January 2021; Received in revised form 6 September 2021; Accepted 8 September 2021

interpolate and geostatistically predict strontium isoscapes for provenance studies in ecological, archaeological, and forensic science (Bartelink and Chesson, 2019; Frei et al., 2020; Koehler et al., 2019; Ladegaard-Pedersen et al., 2020). However, plants, water, and soils can integrate bioavailable strontium at different spatio-temporal scales, which challenges the identification of appropriate substrates (Bataille et al., 2020) and makes it particularly difficult to compare, resemble, and interpolate bioavailable $^{87}Sr/^{86}Sr$ data from multiproxy and intra-site sample variability (Bataille et al., 2020; Bataille and Bowen, 2012; Maurer et al., 2012; Snoeck et al., 2020).

Major advances in strontium isotope sampling strategies and baseline determination have been proposed by manifold authors (Bentley et al., 2004; Hoogewerff et al., 2019; Maurer et al., 2012). For example, Brönnimann et al. (2018) minimized the bias in the data by the integration of a large number and variety of samples, including mineral, botanical, faunal, and human samples from both an archaeological and modern context (Brönnimann et al., 2018). However, limited time availability, financial resources, or access to the data would not allow for fulfilling these requirements. Because human bones, animal dental enamel, and shells are the most common and readily available material on archaeological excavations, this paper aims at presenting a new method for determining strontium isotope baselines based on this restricted sample combination. Due to its high archaeological density, Hungary is particularly well-suited to test and introduce this method.

In this article, a locally variable number of Neolithic human bones, faunal dental enamel, and shells were available per site for strontium isotope baseline determination. To deal with such a challenging dataset and to avoid a combination of baseline samples from various sites exclusively based on geographical proximity and/or geological background data, which would underestimate the small-scale heterogeneity of the environmental settings and the disparities within the surroundings of each individual site (Depaermentier et al., 2020b; Kempf, in preparation, 2020d), we performed comprehensive environmental analyses for the 49 selected Hungarian sites (Fig. 1). If the archaeological context points out that strontium isotope composition of human and animal hard biogenic tissues is related to the isotope composition of

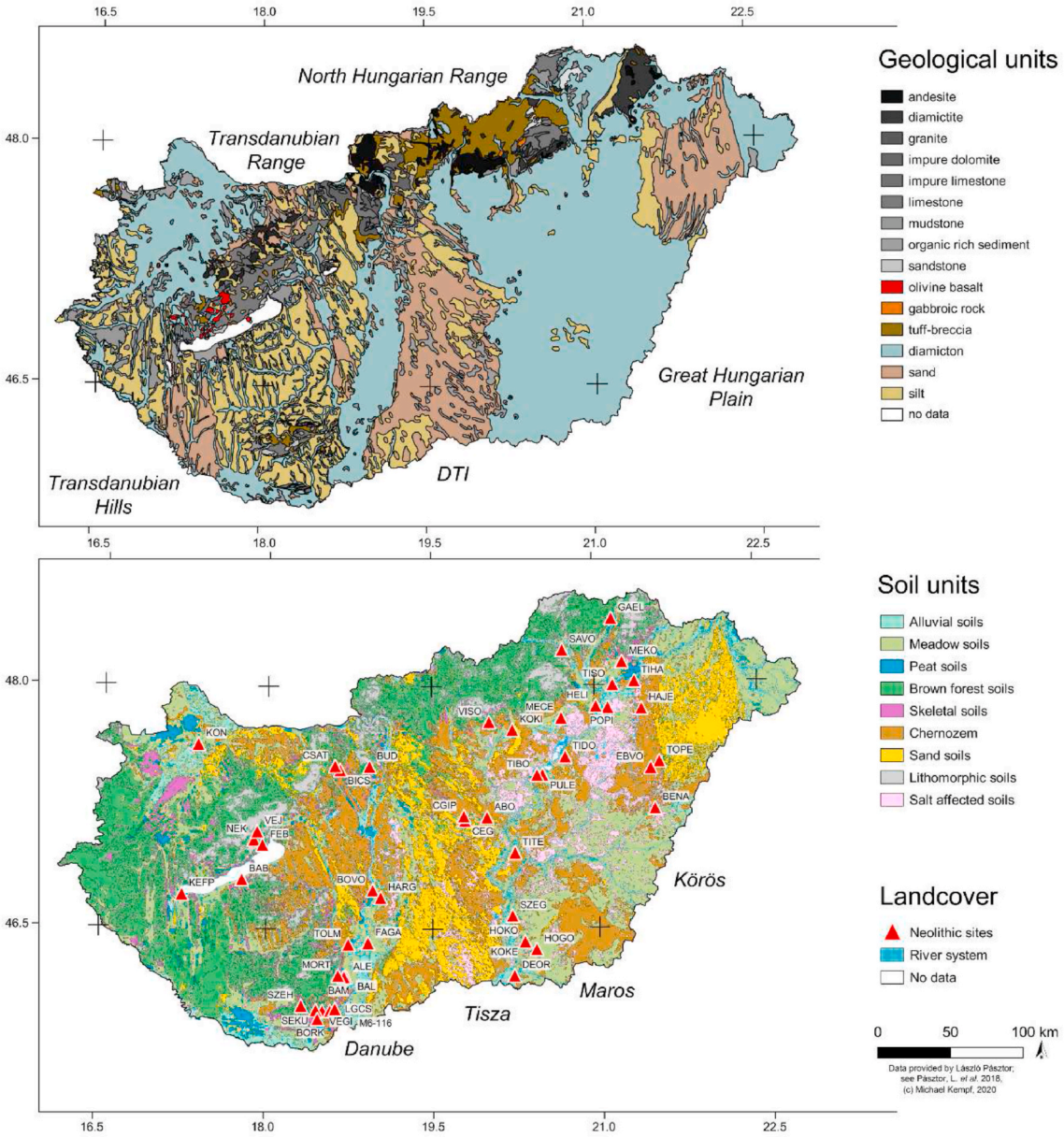

Fig. 1. Geological map and soil units in Hungary including the location of the study sites (EGDI, 2020; Kempf, 2020d; Laborczi et al., 2016; Pásztor et al., 2018). For abbreviations and detailed geological and pedological data, see (Table 1).

consumed food that is overwhelmingly sourced from within the catchment area around a site, we assume that similar environmental settings within that catchment would have led to similar strontium isotope composition. This paper proposes an innovative analytical technique that includes GIS-based, remotely sensed, quantitative and qualitative environmental analyses to determine strontium isotope baselines considering large sample size variability. Applied to provenance and mobility studies, this method enhances the interpretation potential of an individual's local, regional, or supra-regional movement patterns (Depaermentier et al., 2020a; Depaermentier et al., 2020b).

2. Material and methods

2.1. Environmental settings

Hungary is characterized by a moderate continental climate with marine influences and strong precipitation decline towards the central basin (Ács et al., 2015; Demény et al., 2013; Kiss et al., 2015). Large parts of the Great Hungarian Plain (Alföld) are covered with Quaternary fluvial sediments, Pleistocene loess, and massive sand deposits, which separate the major river systems of the north-south draining rivers Danube and Tisza (Fig. 1) (Fitzsimmons et al., 2012; Kercsmár, 2015; Sümegi and Kertész, 2001). Holocene wind erosion, accumulation of sandy deposits (Négyesi et al., 2019; Obreht et al., 2019), and intensive floodplain dynamics throughout the early to the mid-Holocene have continuously altered the landscape composition and the faunal and floral potential habitats (Longman et al., 2019; Tapody et al., 2018). A fragmented landscape with micro-site vegetation refuges and small-scale heterogeneous soil mosaics developed (Birkás et al., 2004; Laborczi et al., 2016; Pásztor et al., 2012, 2018; Várallay, 1989), which control agricultural exploitation, land-use opportunities, and settlement location choice since the early Neolithic period (Depaermentier et al., 2020b; Kempf, in preparation, 2020d; Sherratt, 1983; Sümegi et al., 2013; Whittle et al., 2013). In this specific landscape, loess-covered sediment fans interchange with sandy islands and uneroded palaeolevees across the former floodplain on which hydromorphic alluvial and meadow soils provided potential agricultural cropland and pastures (Sherratt, 1983).

The study area can be distinguished into two major regions, Transdanubia in the western and the Alföld (Great Hungarian Plain) in the eastern part of present-day Hungary (Fig. 1). Geographically, the Alföld belongs to the Southeast European region (including Banat and Voivodina) and the hilly landscapes of Transdanubia are related to the Central European region. However, this division is also largely cultural, since there were strong differences between the cultural groups (and their respective long-distance networks) west of the Danube and east of the Tisza between the 6th and 4th millennium BC (Bánffy, 2013). In this context, the Danube-Tisza Interfluve (DTI) was culturally assigned to Transdanubia. The sandy plateau, however, remained mostly uninhabited during the Neolithic due to the less fertile soils and the decreased environmental location parameters (Bánffy, 2013; Kempf, in preparation, 2020d). Because this study was embedded in a German-Hungarian interdisciplinary research project that aimed to investigate the settlement and population history of the Carpathian Basin in the Neolithic, the distinction between Transdanubia and the Alföld was maintained in this paper.

2.2. Strontium isotope analyses

The isotope ^{87}Sr is formed in the bedrock through the radioactive decay of rubidium (^{87}Rb, t1/2–4.7 × 1010 years) and its concentration in local geology is strongly related to the age and type of the bedrock (Bentley, 2006; Price et al., 2012). The remaining strontium isotopes (^{84}Sr, ^{86}Sr, ^{88}Sr) are non-radiogenic (Price et al., 2004; Price et al., 2002). Strontium becomes biologically available in soil and water trough weathering processes and finally enters the food chain through the vegetation (Bentley, 2006; Montgomery, 2010; Price et al., 2012). When consuming plants, strontium enters human and/or animal metabolisms and gets stored without significant fractionation into their hard mineral tissues as a substitute for calcium (Bentley, 2006; Montgomery, 2010; Price et al., 2002). Consequently, the $^{87}Sr/^{86}Sr$ ratios measured in human and faunal teeth reflect the strontium isotope composition of consumed foodstuffs, which depends on environmental settings and location of the dietary resources (Bentley, 2006; Montgomery, 2010; Price et al., 2012).

In this study, Neolithic human bones (n = 182), archaeological faunal dental enamel (n = 102), and archaeological shells (n = 2 *Gastropoda* and 27 *Bivalvia*)) were sampled for strontium isotope analyses within the various excavation areas (see Data S1). Because human bones are susceptible to diagenetic processes, their strontium isotope composition usually equals the $^{87}Sr/^{86}Sr$ values of the burial soils (Brettell et al., 2012; Knipper, 2004; Price et al., 2002). Sampling the dental enamel of archaeological domestic fauna is further considered a well-suited indicator of the bioavailable strontium but requires an intense knowledge of past husbandry strategies (Brönnimann et al., 2018; Price et al., 2002; Whelton et al., 2018). Mammals with smaller habitats and shells might be more suitable to determine a local baseline (Bentley, 2006; Brönnimann et al., 2018; Slovak and Paytan, 2011). However, snail shells (e.g. *Gastropoda*) can be biased by soil composition or rainwater and consequently show lower $^{87}Sr/^{86}Sr$ ratios than plants or other samples (Evans et al., 2010; Oelze et al., 2012). The bivalve shells, on the other hand, reflect the strontium isotope composition of the freshwater they are coming from (Maurer et al., 2012).

In this case, the composition of each baseline sample depended largely on the preservation and availability of baseline samples. The vast majority of material originated from old excavations and only human bones and occasionally animal remains (not systematically including teeth) were made available for sampling. If possible, long human bones (preferably femura and a few humeri or tibiae), otherwise ribs or other skeletal parts (e.g., skull, pelvis or fibula) were selected for strontium isotope analyses. The faunal sample comprised mostly domesticated species that were expected to be kept close to the Neolithic settlements (*Sus domesticus* and/or *Ovis/Capra*), or other available species (*Bos taurus* or *Canis familiaris*)). However, no rodents were available from the Neolithic sites. If available, samples from wild species (*Cervus elaphus*, and *Sus scrofa*) that could represent the isotopic composition of hunted and gathered food were included. Shells and faunal remains were food leftovers that originated from pits within the Neolithic settlements. They were considered the residues of local freshwater bivalves collected by Neolithic people in local wetlands in the immediate vicinity of the sites. No water, soil, or plant samples were taken due to financial issues and the location of the sites within strongly fertilized areas. The samples were prepared following the methods described by Corina Knipper and colleagues (Knipper et al., 2018). Strontium isotope analyses followed the same methods and techniques described by Corina Knipper et al., 2012 and 2014 (Knipper et al., 2012, 2014) and were conducted at the Curt-Engelhorn-Centre for Archaeometry at Mannheim, Germany.

The baseline samples were inconsistent in type, quantity, excavation period, and sampling techniques. Most of the sites provided archaeological human bones and/or faunal dental enamel samples but shell samples were only available from 15 sites (see Data S1 and Table 2). Furthermore, 15 sites provided only human bones and three sites only faunal dental enamel for the determination of the baseline. Two sites delivered only faunal and shell samples and one site only human bones and shells. Therefore, a total of n = 113 published $^{87}Sr/^{86}Sr$ isotope comparison data (Alt et al., 2014; Gerling et al., 2012; Gerling, 2015; Giblin, 2009; Giblin et al., 2013; Heinrich-Tamáska and Schweissing, 2011; Price et al., 2004; Whittle et al., 2013) were added to our dataset (see Data S2). The in many cases poor quality and quantity of baseline samples per site required the development of a new strategy to combine strontium isotope baseline data from sites with comparable environmental settings.

Table 1
Study sites with geological and pedological conditions.

Region	Site name	Abbr.	Lat	Lon	Soil units	Superficial geology	Main geological unit	Age of the geological unit	Bedrock
Alföld	Abony 60. lh.	ABO	47.19	20.00	sand soil	Fluvial sediments	diamicton	Pleistocene	clastic sediments
	Berettyóújfalu-Nagy-Bócs dűlő	BENA	47.23	21.53	meadow soil	Fluvial sediments	diamicton	Holocene	clastic sediments
	Cegléd	CEG	47.17	19.80	meadow soil	Loess	silt	Pleistocene	mudstone
	Cegled Ipari park	CGIP	47.20	19.79	meadow soil	Loess	silt	Pleistocene	mudstone
	Deszk Ordos	DEOR	46.21	20.23	peat soil	Fluvial sediments	diamicton	Holocene	clastic sediments
	Ebes- Zsong-völgy	EBVÖ	47.48	21.50	Chernozem	Loess	silt	Pleistocene	mudstone
	Garadna- Elkerülö 2.lh	GAEL	48.41	21.17	brown forest soil	Fluvial sediments	diamicton	Pleistocene	clastic sediments
	Hajdunanas-Eszlari ut, M3-45	HAJE	47.85	21.43	Chernozem	Loess	diamicton	Pleistocene	clastic sediments
	Hejökürt-Lidl logisztikai központ	HELI	47.87	21.01	meadow soil	Fluvial sediments	diamicton	Holocene	clastic sediments
	Hódmezővásárhely -Gorzsa V. lh: Homokbànya	HOGO	46.37	20.43	meadow soil	Fluvial sediments	diamicton	Pleistocene	clastic sediments
	Hódmezővásárhely Kotacpart	HOKO	46.42	20.33	meadow soil	Fluvial sediments	diamicton	Pleistocene	clastic sediments
	HMV Kökénydomb	KÖKE	46.42	20.33	meadow soil	Fluvial sediments	diamicton	Pleistocene	clastic sediments
	Kompolt-Kígyós-ér	KOKI	47.73	20.24	meadow soil	Fluvial sediments	tuff-breccia	Miocene	pyroclastic rock
	Mezökeresztes-Cethalom	MECE	47.80	20.69	meadow soil	Fluvial sediments	diamicton	Pleistocene	clastic sediments
	Mezőzombor – Községi temető	MEKÖ	48.14	21.26	meadow soil	Fluvial sediments	diamicton	Pleistocene	clastic sediments
	Polgár-Piócási-Dűlő	POPI	47.86	21.12	brown forest soil	Fluvial sediments	diamicton	Holocene	clastic sediments
	Pusztataksony Ledence	PULE	47.45	20.51	sand soil	Fluvial sediments	diamicton	Holocene	clastic sediments
	Szegvár Tűzköves	SZEG	46.03	20.22	alluvial soil	Fluvial sediments	diamicton	Pleistocene	clastic sediments
	Tiszabura Bonishat	TIBO	47.56	20.46	sand soil	Fluvial sediments	diamicton	Holocene	clastic sediments
	Tiszaszőlős - Domaháza-puszta, Réti-dűlő	TIDO	48.02	20.72	alluvial soil	Fluvial sediments	diamicton	Holocene	clastic sediments
	Tiszalök Hajnalos	TIHA	48.00	21.37	meadow soil	Loess	silt	Pleistocene	mudstone
	Tiszadob-Okenéz	TISO	46.97	21.17	alluvial soil	Fluvial sediments	diamicton	Holocene	clastic sediments
	Tiszaföldvár Téglagyár	TITE	46.97	20.25	meadow soil	Fluvial sediments	diamicton	Holocene	clastic sediments
	Debrecen Tócópart Erdöalja	TOPE	47.52	21.58	meadow soil	Loess	silt	Pleistocene	mudstone
	Visonta	VISO	47.78	20.03	meadow soil	Fluvial sediments	diamicton	Pleistocene	clastic sediments
Transdanubia	Alsónyék elkerülö 2. lh.	ALE	46.20	18.72	meadow soil	Fluvial sediments	diamicton	Holocene	clastic sediments
	Balatonszemes Bagódomb	BAB	46.81	17.78	meadow soil	Loess	silt	Pleistocene	mudstone
	Bátaszék, Lajvérpuszta	BAL	46.20	18.70	meadow soil	Fluvial sediments	diamicton	Holocene	clastic sediments
	Bátaszék-Mérnöki telep	BAM	46.21	18.71	meadow soil	Fluvial sediments	diamicton	Holocene	clastic sediments
	Bicske Galagonyás	BICS	47.49	18.66	salt affected soil	Fluvial sediments	diamicton	Holocene	clastic sediments
	Borjád Kenderföldek	BORK	45.94	18.47	meadow soil	Loess	silt	Pleistocene	mudstone
	Bölcske Gyürüsvölgy M3-TO 14. lh.	BÖVÖ	46.74	18.96	sand soil	Fluvial sediments	diamicton	Pleistocene	clastic sediments
	Budakeszi 8. lh. Szőlőskert-Tangazdaság	BUD	47.51	18.93	brown forest soil	Weathered limestone	impure limestone	Eocene	limestone
	Csabdi Télizöldes	CSAT	47.51	18.62	brown forest soil	Loess	silt	Pleistocene	mudstone
	Fajsz	FAGA	46.42	18.92	alluvial soil	Fluvial sediments	diamicton	Holocene	clastic sediments
	Felsőörs-Bárókert	FEB	47.02	17.96	brown forest soil	Weathered limestone	limestone	Triassic	limestone
	Harta-Gátőrház	HARG	46.70	19.03	Chernozem	Fluvial sediments	diamicton	Holocene	clastic sediments
	Keszthely-Fenékpuszta Pusztaszentegyházi dűlő	KEFP	46.71	17.24	meadow soil	fluv./limn. sediments	org. rich sediment	Holocene	clastic sediments
	Kóny 85 Enese	KON	47.64	17.36	meadow soil	Fluvial sediments	diamicton	Holocene	clastic sediments
	Lánycsók Gata Csatola	LGCS	46.01	18.62	meadow soil	Loess	silt	Pleistocene	mudstone
	Lanycsók Csata alja		46.00	18.58	Chernozem		diamicton	Holocene	

(*continued on next page*)

Table 1 (*continued*)

Region	Site name	Abbr.	Lat	Lon	Soil units	Superficial geology	Main geological unit	Age of the geological unit	Bedrock
		M6-116				Fluvial sediments			clastic sediments
	Mórágy Tűzkődomb B1	MORT	46.21	18.65	brown forest soil	Loess	silt	Pleistocene	mudstone
	Nemesvámos-Kapsa	NEK	47.05	17.88	brown forest soil	Loess	silt	Pleistocene	mudstone
	Szederkèny-Kukorica-dülö, 95. lh.	SEKU	46.58	20.71	meadow soil	Loess	silt	Pleistocene	mudstone
	Szemely-Hegyes M60/83. lh.	SZEH	47.45	18.32	brown forest soil	Loess	silt	Pleistocene	mudstone
	Tolna-Mözs TO 003	TOLM	46.41	18.74	Chernozem	Loess	silt	Pleistocene	mudstone
	Versend-Gilencsa	VEGI	46.00	18.51	Chernozem	mudstone	silt	Tortonian	clastic sediments
	Veszprém-Jutasi-Munkacsy út	VEJ	47.01	17.91	brown forest soil	Loess	silt	Pleistocene	mudstone

2.3. Environmental data sources and analyses

The composition of the bioavailable strontium depends on the environmental settings and it can vary strongly on the local scale (Bentley, 2006; Montgomery, 2010; Price et al., 2012; Snoeck et al., 2020). A qualitative multicriteria landscape analysis was conducted to identify those sites that represent comparable environmental settings within their catchment area. Similar settings would lead to comparable bioavailable strontium isotope compositions. The analyses and environmental modelling were carried out using QGIS (QGIS Geographic Information System. QGIS Association, http://www.qgis.org), R software (R: A language and environment for statistical computing. R Foundation for Statistical Computing, Vienna, Austria, https://www.R-project.org/), and remote sensing software (SNAP 6.0; multispec 2018.05.21). Elevation data were downloaded from the USGS (ASTER GDEM is a product of METI and NASA) and hyperspectral satellite imagery was obtained from the ESA Copernicus open access hub and spectrally modified using the red and near infrared channels (Tucker, 1979). Geological datasets were processed from the European Geological Data Infrastructure (EGDI). Digital soil data were provided by László Pásztor from the Hungarian Institute for Soil Science and Agricultural Chemistry at the Hungarian Academy of Sciences, Budapest, Hungary (Bozán et al., 2018; Laborczi et al., 2016; Laborczi et al., 2019; Pásztor et al., 2018; Pásztor et al., 2015a; Pásztor et al., 2015b) and the Corine Landcover (CLC) datasets were used to estimate potential flooding areas. From the datasets, the landscape permeability was calculated using the digital terrain model and the hydrologic data attributes (Howey, 2011; Kempf, 2019, 2020a; Laabs and Knitter, 2021; Nakoinz and Knitter, 2016). Based on an accumulative friction surface, the accessibility of each site catchment was estimated within a radius of up to 5 km, which can be considered a representative and cost-effective settlement catchment average for Neolithic sites in the Carpathian Basin (Kempf, in preparation, 2020d). Slope gradient, potential flooding vulnerability, and potential agricultural suitability based on soil properties were evaluated to compose probability maps for each site catchment and to predict potential land-use, crop cultivation, and extent of pastures for livestock breeding. To test the hypothesis that the geographical proximity of sites is not a sufficient argument for combining samples from various sites for baseline determinations, we compared the $^{87}Sr/^{86}Sr$ values of different areas from the macro-regional (Transdanubia vs. Alföld) to the site-specific scale. The second hypothesis is that the geological background is not a sufficient argument to combine samples from different sites for the determination of the baseline (see also Snoeck et al., 2020). To evaluate that, we compared the $^{87}Sr/^{86}Sr$ values of each sample originating from the same geological unit. The consideration of a broad variety of environmental parameters (Kempf, in preparation, 2020d; Laborczi et al., 2016; Pásztor et al., 2018) in the analysis allowed to distinguish sites with different environmental compositions and to combine similar catchments for the determination of shared strontium isotope baselines.

2.4. Strontium isotope baseline determination

First, a site-specific baseline range was calculated from the mean value of the baseline samples $^{87}Sr/^{86}Sr$ ratios ±2 standard deviations deriving from sites with a large number and variety of baseline samples and/or from sites with comparable environmental settings (Table 2, see also Fig. S1-S32). Even though we assumed that the faunal and shell samples were originating from the local catchment area around the sites, either short- and/or long-distance animal trade can still be expected during the Neolithic (García-Suárez et al., 2020; Munro and Stiner, 2020; Scheu, 2018). Consequently, the possibility that extreme values in animal dental enamel $^{87}Sr/^{86}Sr$-ratios can be related to animal trade cannot be excluded with absolute certainty. In contrast, the *Spondylus* sample from Mórágy – Tűzkődomb (MORTM) was excluded from the baseline determination because it was identified as an import good from the archaeological context. To avoid the inclusion of biased samples in this calculation, single samples exhibiting an isotope ratio, which was considerably above or below the limits of the site-specific baseline range were excluded.

No site-specific strontium isotope baseline was suggested for sites, which neither provided enough baseline data nor could be combined with other sites based on similar environmental conditions. The large number of sites considered in this study and their spatial distribution allowed to determine an additional micro-regional baseline range. This micro-regional baseline range was calculated from the mean value of every baseline sample's strontium isotope ratio ±2 standard deviations in a given geographical area (Table 2). The site combination suggested in this paper for the micro-regional scale is based on site vicinity. The size of the *micro-region* or the number of sites included in it does not correspond to site density analyses or a particular metric system. This represents a more flexible concept that can be adapted to various research areas, sample sizes, and research questions in future projects. The establishment of micro-regional baselines is rather an attempt to add a further spatial dimension to the determination of strontium isotope baselines and the scales of mobility patterns in prehistory. According to this approach, we suggest distinguishing an isotopic signal related to local agricultural practices (site-specific baseline range) from the isotopic range of a larger surrounding area (micro-regional baseline range). Previous results allowed to identify individual mobility patterns on different spatial scales (Depaermentier et al., 2020a; Depaermentier et al., 2020b). Eventually, the isotopic baseline ranges were plotted with their geographical position in order to produce the first strontium isomap of Hungary. The baseline ranges were not interpolated so as to avoid creating hypothetical isotope values at places that did not provide baseline samples.

Table 2
Number of samples per sites and site-specific and micro-regional strontium isotope baseline ranges.

Region	Site	Abbr.	Number of samples per site/comparison data				Site-specific scale			Micro-regional scale		
			Human bones	Animal dental enamel	Shells	Comparison data	87Sr/86Sr mean	SD	Site-specific baseline range	87Sr/86Sr mean	SD	Micro-regional baseline range
Transdanubia	Kóny 85 Enese	KON	1	3	4	no	0.7099	0.0001	0.70970–0.71004	_	_	_
	Lanycsók Csata alja	CSAT	18	0	0	no	0.7090	0.0001	0.70875–0.70928	_	_	_
	Bicske Galagonyás	BICS	3	0	0	no				_	_	_
	Budakeszi 8. lh. Szőlőskert-Tangazdaság	BUD	7	6	0	yes	0.7091	0.0002	0.70861–0.70957	0.7092	0.0003	0.70844–0.70989
	Veszprém-Jutasi-Munkacsy út	VEJ	4	3	0	no	0.7095	0.0004	0.70882–0.70988	0.7096	0.0005	0.70871–0.71051
	Nemesvámos-Kapsa	NEK	1	0	0	no						
	Felsőörs-Bárókert	FEB	3	3	0	yes	0.7098	0.0005	0.70887–0.71067			
	Balatonszemes Bagódomb	BAB	3	3	0	yes	0.7093	0.0002	0.70878–0.70984	_	_	0.70878–0.71000
	Keszthely-Fenékpuszta Pusztaszentegyházi dűlő	KEFP	4	0	0	yes	0.7095	0.0001	0.70918–0.70975	_	_	0.70874–0.70975
	Harta-Gátőrház	HARG	3	3	0	yes	0.7091	0.0001	0.70875–0.70962	0.7092	0.0002	0.70884–0.70961
	Fajsz	FAGA	2	0	0	yes						
	Bölcske Gyürüsvölgy M3-TO 14. lh.	BÖVÖ	3	3	2	no	0.7093	0.0002	0.70890–0.70968			
	Tolna-Mözs TO 026	TOLM	2	2	0	no	0.7092	0.0001	(0.70910–0.70937)			
	Alsónyék elkerülö 2. lh.	ALE	0	4	1	no	0.7093	0.0003	(0.70877–0.70987)	0.7097	0.0003	0.70901–0.71034
	Bátaszék, Lajvérpuszta	BAL	7	2	0	no	0.7098	0.0003	0.70927–0.71032			
	Bátaszék-Mérnöki telep	BAM	0	4	2	no						
	Mórágy Tűzkődomb B1	MORT	8	4	1	no	0.7097	0.0003	0.70887–0.71036			
	Lánycsók Gata Csatola	LCGS	0	3	0	no	(0.7097)	(0.0001)	_	0.7097	0.0001	0.70939–0.70994
	Lanycsók Csata alja	M6-116	4	2	0	no	0.7099	0.0001	0.70955–0.71015			
	Versend-Gilencsa	VEGI	7	4	0	no	0.7097	0.0001	0.70945–0.70995			
	Szederkèny-Kukorica-dülö 95. lh.	SEKU	6	0	0	no	0.7095	0.0000	(0.70948–0.70959)			
	Borjád Kenderföldek	BORK	1	0	0	no						
	Szemely-Hegyes M60/83. lh.	SZEH	5	3	2	no	0.7097	0.0001	0.70971–0.70998			
Alföld	Sajoszentpeter-vasúti örhaz	SAVÖ	0	0	0	no	_	_	_	_	_	_
	Garadna- Elkerülö 2.lh	GAEL	4	3	1	no	0.7110	0.0002	0.71048–0.71161	_	_	_
	Visonta	VISO	1	0	0	no	_	_	_	_	_	_
	Kompolt-Kígyós-ér	KOKI	2	2	0	yes	0.7109	0.0001	0.71067–0.71117	_	_	0.70920–0.71117
	Mezökeresztes-Cethalom	MECE	4	4	2	yes	0.7010	0.0001	0.70983–0.71015	_	_	0.70920–0.71027
	Hajdunanas-Eszlari ut, M3-46	HAJE	6	4	1	no	0.7098	0.0002	0.70949–0.71015	0.7099	0.0003	0.70929–0.71056
	Tiszalök Hajnalos	TIHA	1	0	0	no	_	_	_			
	Hejökürt-Lidl logisztikai központ	HELI	5	5	3	no	0.7104	0.0001	0.71006–0.71077			
	Polgár-Piócási-Dűlő	POPI	4	0	0	yes	0.7098	0.0001	0.70969–0.70994			
	Tiszadob-Okenéz	TISO	5	3	0	no	0.7095	0.0001	0.7094–0.70962			
	Mezőzombor – Községi temető	MEKÖ	4	3	3	no	0.7101	0.0001	0.70988–0.71032			
	Tiszabura Bonishat	TIBO	2	0	1	yes	_	_	_	0.7096	0.0001	0.70937–0.71000
	Tiszaszőlős - Domaháza-puszta, Réti-dűlő	TIDO	0	2	0	yes	0.7096	0.0001	0.70939–0.70983			
	Pusztataksony Ledence	PULE	9	6	2	yes						
	Abony 60. lh.	ABO	8	4	0	no	0.7092	0.0001	0.70904–0.70938	0.7093	0.0002	0.70894–0.70960
	Tiszaföldvár Téglagyár	TITE	3	0	0	no	(0.7095)	(0.0001)	(0.70940–0.70960)			
	Cegléd	CEG	6	2	2	no	0.7094	0.0001	0.70931–0.70958	0.7096	0.0003	0.7090–0.71025
	Cegléd Ipari park	CGIP	4	0	0	no	(0.7101)	(0.0001)	(0.70997–0.71022)			
	Debrecen Tócópart Erdöalja	TOPE	2	4	0	yes	0.7099	0.0001	0.70984–0.71004	_	_	0.709–0.711 (Gerling, 2015)
	Ebes-Zsong-völgy	EBVÖ	3	0	2	yes	0.7010	0.0003	0.70984–0.71042	_	_	
	Berettyóújfalu-Nagy-Bócs dűlő	BENA	1	2	0	yes	(0.7102)	(0.0002)	(0.70961–0.71082)	_	_	
	Szegvár Tűzköves	SZEG	1	0	0	no	_	_	_	0.7095	0.0002	0.70928–0.70976
	Hódmezővásárhely Kotacpart	HOKO	2	3	0	no	_	_	_			
	Hódmezővásárhely-Gorzsa V. lh Homokbànya	HOGO	1	0	0	no	_	_	_			
	HMV Kökénydomb	KÖKE	2	0	0	no	_	_	_			
	Deszk Ordos	DEOR	0	3	0	no	_	_	_			

3. Results

3.1. Strontium isotope analyses

The $^{87}Sr/^{86}Sr$ ratios of the diverse baseline samples varied from 0.70866 to 0.71147 with a mean value of 0.70967 (SD = 0.0005) throughout Hungary (see Fig. 2 and Data S1). The measurements of the international standard for $^{87}Sr/^{86}Sr$ (NBS 987) gave a mean value of 0.71020 ± 0.00004 (1 SD, n = 23), which fits well with the expected value of 0.71034 ± 0.00026 (with a confidence interval of 95%) (National Institute of Standards & Technology, 2007). The Eimer & Amend (E & A) standard yielded $^{87}Sr/^{86}Sr$ ratios of 0.70800 ± 0.00006 (1 SD; n = 251), which also fits the expected value of 0.708027 ± 0.000035 (1 SD) (Müller-Sohnius, 2007). The variability of the strontium isotope composition mirrors the geographical heterogeneity of the Carpathian Basin, and the data follow roughly a normal distribution ($R^2 = 0.9635$), although some extreme values were identified (Fig. 3). A first trend can be observed on the large-scale as demonstrated by the generally lower $^{87}Sr/^{86}Sr$ ratios of Transdanubia compared to the Alföld (Fig. 4). A two-sample Kolmogorov-Smirnov test showed that the values were not drawn from the same distribution (p-value = 1.234e-07). On the regional scale, the data can be divided into smaller units, which show intra-regional comparable geographical settings as well as inter-regional disparities in $^{87}Sr/^{86}Sr$ data (Fig. 4). An ANOVA test for variance and a TukeyHSD (Tukey, 1977) test for micro-regional site variability have been performed (R Core Team and contributors worldwide, 2021). The ANOVA gives a F-value of 45.54 and a p-value of nearly 0 (<2e-16 ***), which rejects the null hypothesis of no difference between the group means of the sample regions. Although we can reject the null hypothesis, we cannot determine which groups are different (Haynes, 2013). To avoid the multiple comparison problem of single *t*-test combinations, we applied Tukey's honest significant differences, which takes multiple comparisons into account and determines 0.05 as significant difference. The plot (see Fig. S33) visualizes the confidence levels with the horizontal line crossing the vertical dashed line indicating no significant difference (see also Data_S3) (Carlson, 2017). From the plots, we can see large heterogeneity of all sites with most sites showing micro-regional variability. A third trend demonstrates that small-scale environmental heterogeneity can lead to further disparities on the site-specific scale (Figs. 2 and 6; Fig. S1-S32). Similar environmental settings led to similar isotope ranges and different environmental settings were occasionally characterized by distinct isotopic composition. This applied most of the Alföld sites (see Fig. S19-S20 and S25-S32) and a few sites in Transdanubia (see Fig. S6-S10) In two cases (MORT compared to ALE-BAL-BAM, and VISO compared to KOKI), however, considerably different settings led to similar strontium isotope values.

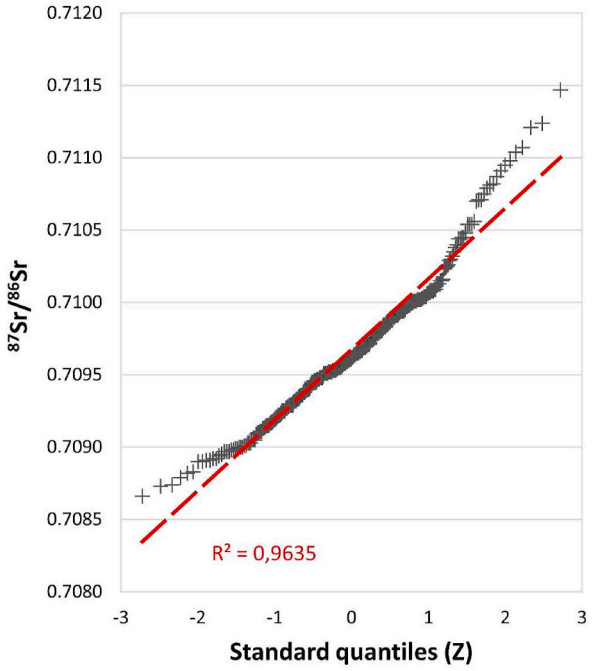

Fig. 3. The data follow a normal distribution ($R^2 = 0.9635$). A few extreme values can be identified.

Most of the sites are situated either on fluvial deposits (diamicton) or silt (loess). The soil compositions are mostly characterized by alluvial and meadow soils or Chernozem soils (Table 1) (Kempf, 2020d). Due to their scattered origin, the long-distance transport, and the heterogeneous composition of the fluvial sediments and the loess deposits, the sites provided highly variable strontium isotope values (Fig. S34).

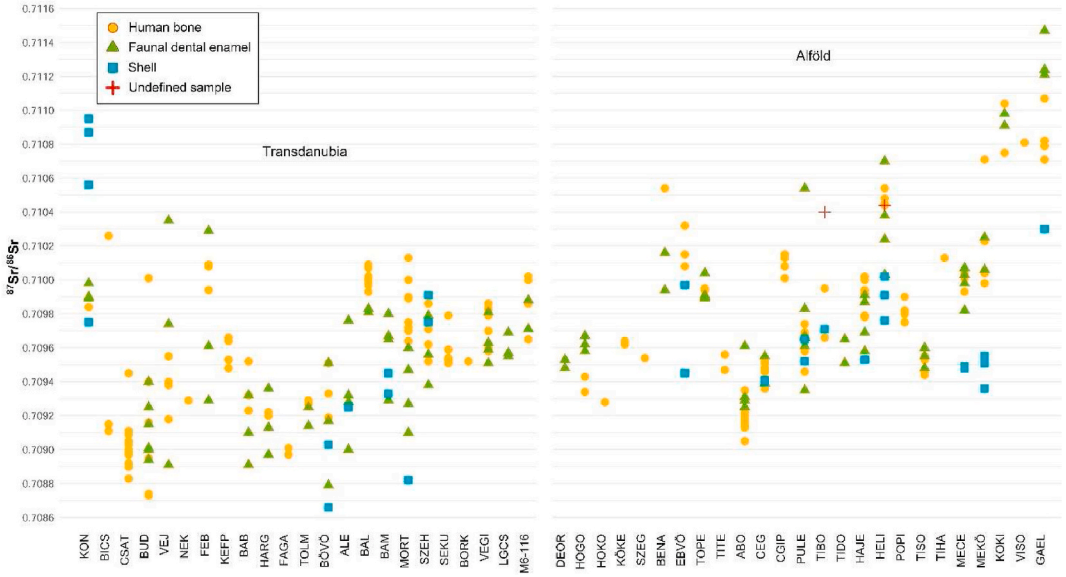

Fig. 2. $^{87}Sr/^{86}Sr$ ratios of each baseline sample per site and by type. Yellow dots = human bones; green triangles = faunal dental enamel; blue squares = shell samples; red crosses = undefined samples. The sites are arranged in a continuous geographical order: Transdanubia (north to south), Alföld (south to north). (For interpretation of the references to colour in this figure legend, the reader is referred to the Web version of this article.)

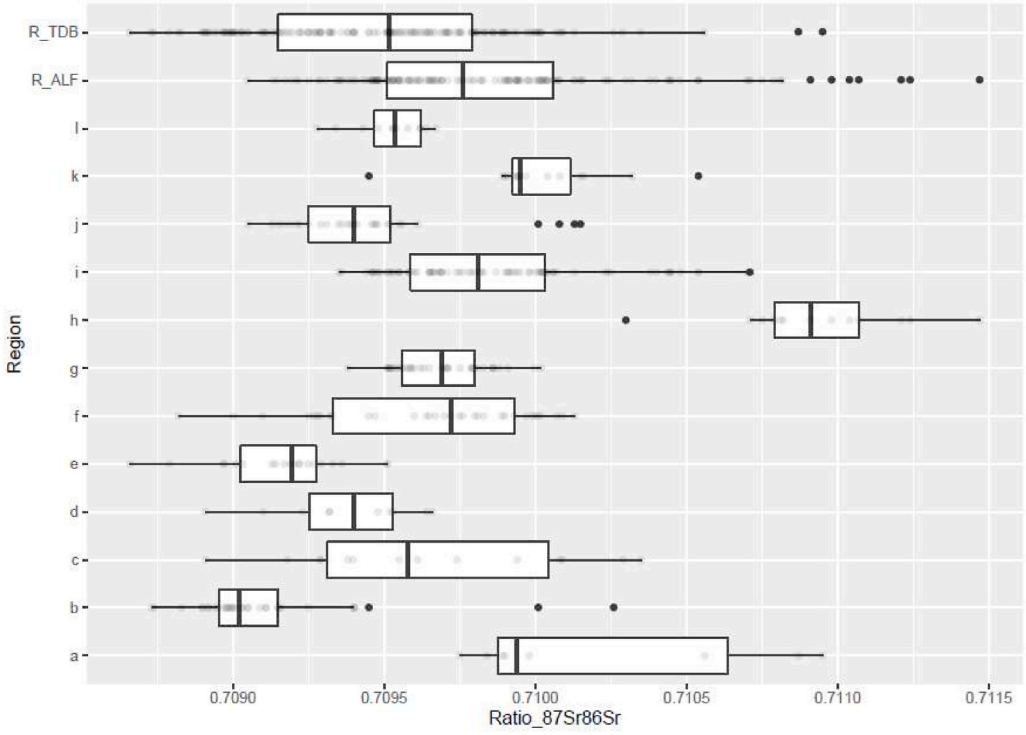

Fig. 4. Boxplots of regional (Transdanubia (TDB), Alföld (ALF)) and micro-regional (a–l) $^{87}Sr/^{86}Sr$ ratios: Strontium isotope ratios in Transdanubia are generally lower than in the Alföld; a: Northern Transdanubia (KON); b: Budapest-region. c: Bakony Mountains; d: South of the Lake Balaton; e: Fajsz-Harta region; f: Alsónyék-Bátaszék region; g: Southern Transdanubia; h: Northern Alföld (mountains); i: Northern Tisza-region; j: Cegléd-Abony region; k: Sárrét region; l: Southern Alföld. Boxplots created using the ggplot2 package (Wickham, 2016) and R-software.

Despite the significant difference in mean values (Welch two sample *t*-test: p-value = 3.982e-06) and the narrower bandwidth of strontium isotope values from silt compared to the fluvial sediments (Two-sample Kolmogorov-Smirnov test: p-value = 0.008369), which could be due to the generally lower sample number, Fig. 5 and Fig. S34 illustrate the overlap of strontium isotope values from silt and diamicton. The other geological units did not provide enough samples for a representative comparison and statistical analysis. However, there is a tendency for limestone and organic rich sediment to show similar $^{87}Sr/^{86}Sr$ ratios compared to the ratios of diamicton and silt. The four samples from volcanic tuff breccia show generally higher values. Concluding from this, the various geological units do not demonstrate specific bioavailable strontium isotope composition. This further highlights the importance of multiproxy environmental models to determine local strontium isotope baseline ranges.

The isotope composition of different sample types occasionally demonstrated distinct ranges (Fig. S35 and S36). At ABO, ALE-BAL-BAM, GAEL, MORT, KON, and TOLM, the human bones and faunal dental enamel $^{87}Sr/^{86}Sr$ ratios were largely distinct and there was only slight overlap at BAB, HAJE, TISO, and TOPE. At the other sites, the strontium isotope values of human bones largely overlapped with those of the faunal dental enamel. However, at BÖVÖ, FEB, NEK-VEJ, HELI, and MECE, the human bones showed a narrower range and at BUD, M6-116, KOKI, MEKÖ, and DEOR-KÖKE-HOGO-HOKO-SZEG, they showed a

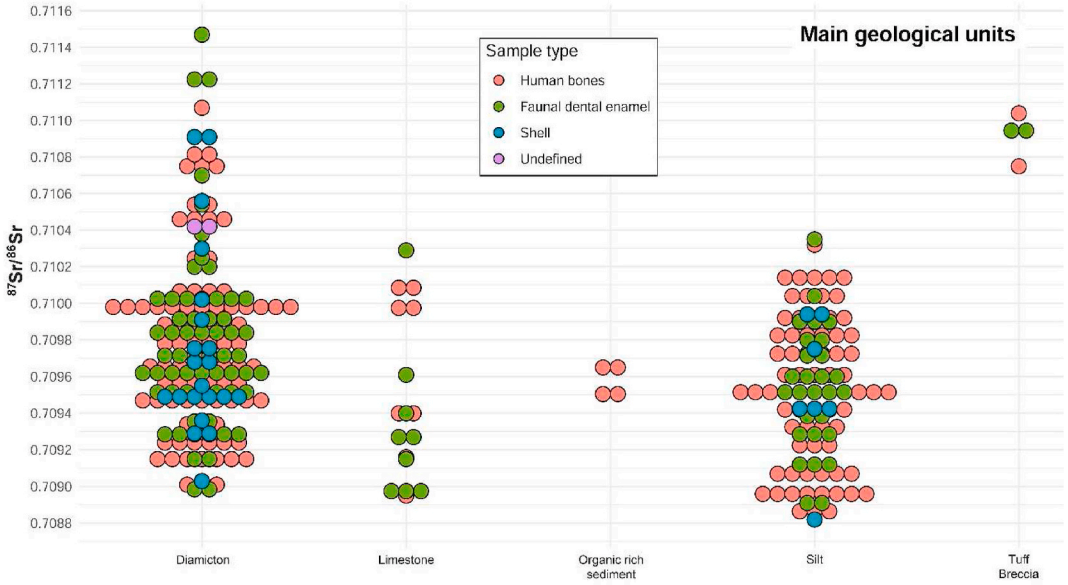

Fig. 5. $^{87}Sr/^{86}Sr$ ratios of the various baseline sample types collected from distinct geological units. Diamicton and silt are the most frequent geological units within the site catchment areas, and they provided similar strontium isotope values.

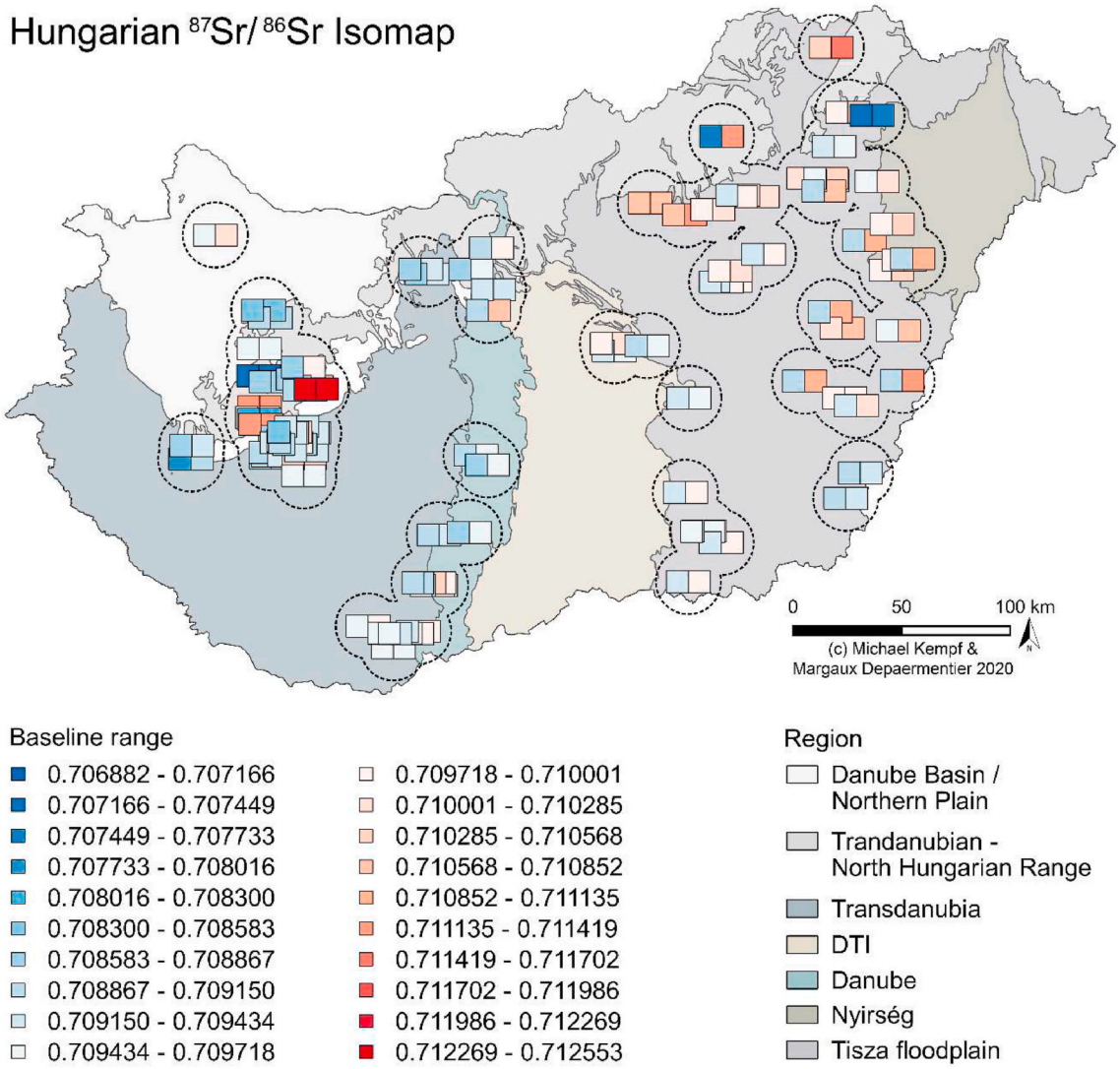

Fig. 6. a. Hungarian strontium isomap. The strontium isotope baseline ranges of 49 Neolithic sites (see Table 1 for the abbreviations) and additional isotopic comparison data (see Data S2 for the abbreviations) were mapped with the values of the upper and lower limits of the site-specific baseline range (see Data S1 for individual sample data and Table 2 for individual baseline ranges). Due to a locally high site density and graphic overlaps, the regions are split in Fig. 6b and c. A high resolution of this isomap is provided in the supplement (Fig. S37). b. Strontium isotope baseline ranges for the regions Danubian Basin/Northern Plain, DTI, Transdanubia, and the Danube floodplain. The Northern Plain and the DTI show a low number of sites (KON, CGIP and CEG) and isotope comparison sites (1, 3) (see Table 1 and Data S2 for the list of the abbreviations). A high resolution of this isomap is provided in the supplement (Fig. S38). c. Strontium isotope baseline ranges for the regions Transdanubian/Northern Range, the river Tisza floodplain and the Nyirség. The river Tisza floodplain shows strontium baseline range values that alter from the north to the south according to the change in the sedimentation regime of the river Tisza and the tributaries. The region Nyirség only features four sites that are similar to the floodplain baseline ranges due to the comparable geological signal of the alluvial sediments (see Table 1 and Data S2 for the list of the abbreviations). A high resolution of this isomap is provided in the supplement (Fig. S39).

larger range compared to the faunal dental enamel. This could illustrate that human bones and faunal samples generally provide complementary isotope data, although it is important to consider the species habitat variability represented by the faunal samples. In this study, however, the number of samples from different animal species by site was too low to consider the species separately. More than half of the shells included in this research showed considerably different values compared to the other samples and had to be considered as outliers. Only the shells from ALE-BAL-BAM, BÖVÖ, CEG, PULE-TIDO, and TIBO had a similar strontium isotope composition than the other baseline samples. The results of the Pearson correlation analysis showed no correlation between the large number of outlier shells and the preparing methods. The same applies to the Sr ppm value, the soil units, and the respective geological units (see Data_S4).

It was possible to determine a site-specific and a micro-regional strontium isotope baseline range for most of the sites (see Fig. S1-S31). At ten sites it was not possible to determine a representative site-specific baseline range, because they did not provide enough baseline samples and could not be combined with other sites based on the multicriteria environmental analyses. In nine of these cases, only a micro-regional isotopic range was suggested. For Visonta (VISO), no reliable site-specific or a micro-regional baseline was determined, which is due to the distance to the next comparison sites (Table 2). The baseline ranges were mapped with the $^{87}Sr/^{86}Sr$ value of the upper and lower limits of the site-specific (if necessary, the micro-regional) strontium isotope baseline range to produce a comparable strontium isomap for Hungary. Due to the heterogeneous environmental composition of Hungary, a differentiation into seven subregions increases the

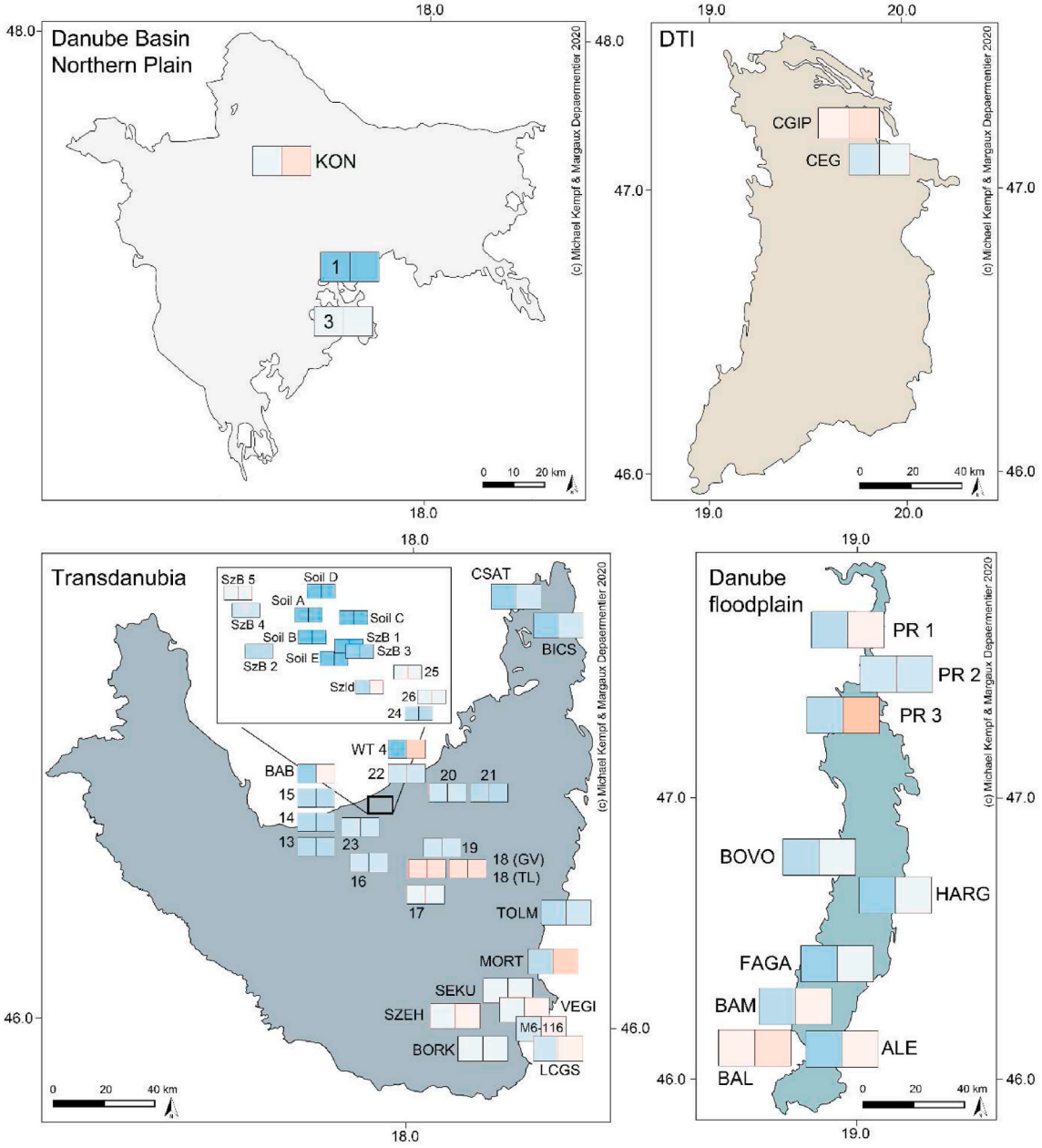

Fig. 6. (*continued*).

visualization of the regional isotope baseline ranges (Fig. 6a). Detailed macro-regional classifications resulting from environmental and isotope analyses are presented in Fig. 6b and c.

4. Discussion

4.1. Strontium baseline sample variability

In this study, Neolithic human bones, faunal dental enamel, and shells were sampled for strontium isotope analyses from various excavation sites. The number and variety of the samples depended on the preservation and availability of potential baseline samples at the site, which led to frequently small and/or inconsistent samples per site (see Data S1). Because of the porosity of the tissues, bone strontium isotope composition can change rapidly after deposition due to physical weathering processes (Nelson et al., 1986; Trueman, 2004; Trueman et al., 2004; Trueman and Tuross, 2002). Therefore, human bones are often used as a proxy for the strontium isotope value of the local soil (Brettell et al., 2012; Knipper, 2004; Price et al., 2002; Trickett et al., 2003). Based on the continuous remodelling and turnover of bone tissues, a different approach suggests that particularly well preserved or cleaned bones are not contaminated and hence can represent an average strontium isotope value of the individual's diet during the last few years of life (Knudson et al., 2012; Price et al., 2002; Price et al., 2000; Schweissing and Grupe, 2003). In this context, the ribs would represent approximately the last five years of life, while the thicker bones such as the femora or the pelvis would represent an average value of the last decades before death due to different turnover rates (Price et al., 2000). The strontium isotope composition of the teeth characterises the childhood and the composition of the bone is considered to represent the diet and consequently the mobility of the last years before death (Knudson et al., 2012; Price et al., 2002; Price et al., 2000; Schweissing and Grupe, 2003). Frequently, however, the proportion of local bones is surprisingly high, giving the impression that circulating soil water *actually* has a

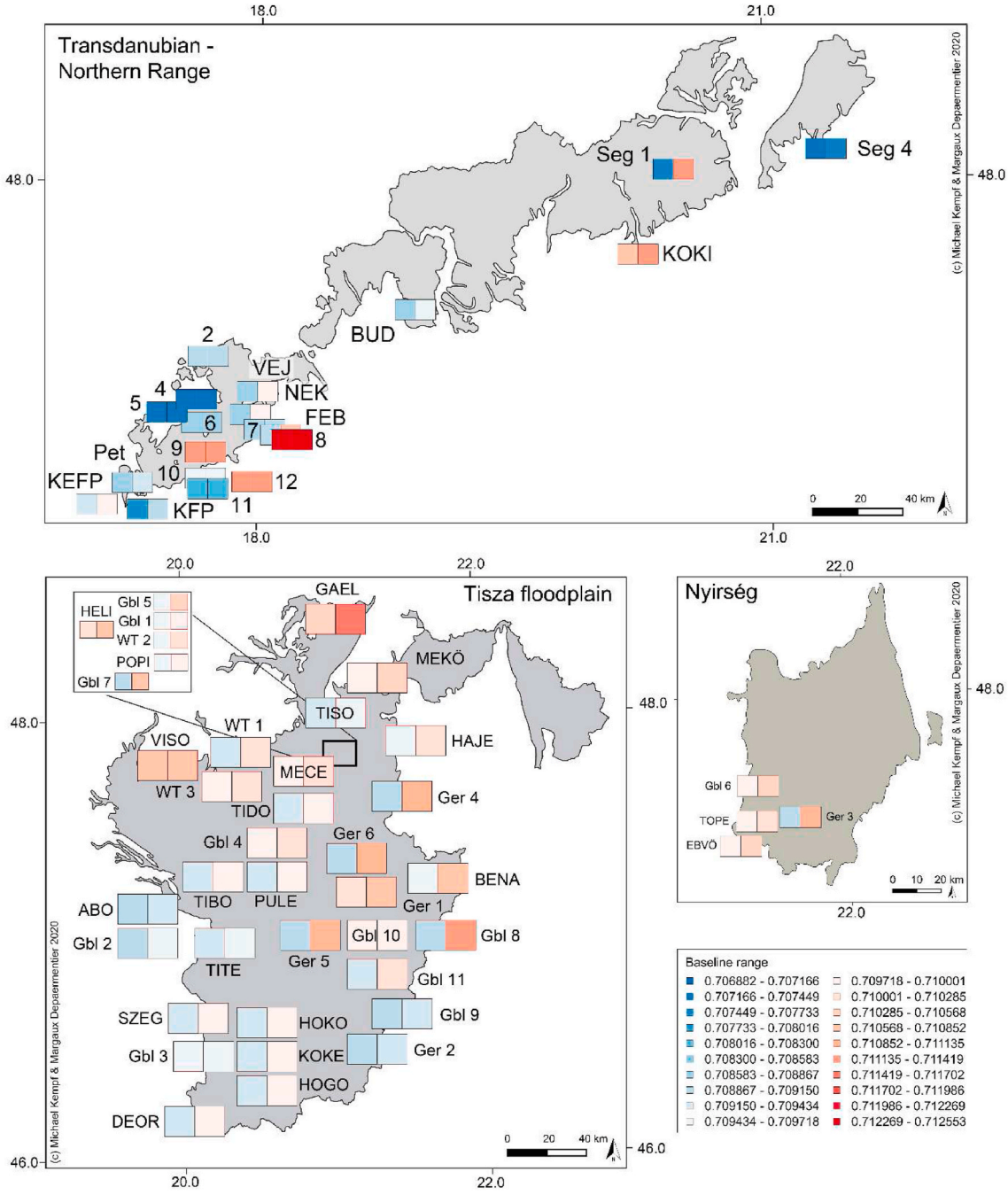

Fig. 6. (*continued*).

considerable impact on the strontium composition of the deposited material. A difference between the bone and the bedrock or the soil strontium isotope value is thus both considered as an evidence for no contamination of the bone and for a late mobility of the individual (Grupe et al., 1997; Knudson et al., 2012; Kulp and Turekian, 1956). In this study, we assumed that the Neolithic bones were altered enough to have taken up the strontium isotope values of the surrounding soil and water, but further analyses would be required to confirm that their strontium isotope composition completely equilibrated.

Moreover, the isotope composition of different sample types occasionally demonstrated distinct ranges (Fig. S35-S36). The fact that the human bones from BÖVÖ, FEB, NEK-VEJ, HELI, and MECE showed narrower ranges than the faunal dental enamel, could demonstrate that – depending on the heterogeneity and the extent of the potential cropland in the catchment around a settlement – the very local soil signal of the burial pit cannot be considered representative for the entire human activity range (Kempf, 2020d). However, this cannot be assumed consistently for the entire study area, because human bones from BUD, DEOR-KÖKE-HOGO-HOKO-SZEG, KOKI, MEKÖ, and M6-116 showed a larger range than the faunal dental enamel. This rather mirrors micro-scale variations in soil composition (Brettell et al., 2012; Knipper, 2004; Price et al., 2002). *Sus domesticus* and *Ovis/Capra* were preferably sampled since there is no evidence for extensive pastoralism or nomadism for these sites. Recent studies conducted at other Neolithic sites showed that cattle was usually kept farther away from the settlement (García-Suárez et al., 2020; Stiner et al., 2014; Vaiglova et al., 2018). This hypothesis was not supported by our data, because the $^{87}Sr/^{86}Sr$ values from *Bos taurus* dental enamel at BUD and KOKI did not differ from the other samples. Due to the small number of species samples at the different sites, it was not possible to define more precise

husbandry practices from the dataset. The usual overlap of the strontium isotope ranges of human bones and faunal dental enamel (Fig. S35-S36) generally showed complementary results within Neolithic site-catchment areas.

In most cases, the shells sampled for this study exhibited distinct $^{87}Sr/^{86}Sr$ ratios compared to the other samples from the same sites (Fig. S35-S36). That could be explained by diagenetic processes, particularly for the two *Gastropoda* (Evans et al., 2010; Oelze et al., 2012). The strontium isotope composition of the bivalve shell's hydrologic environment presents a mixed value of various geological units, which is not representative for the site-specific strontium isotope composition (Maurer et al., 2012). The outlier data were therefore excluded from the calculation of the baseline according to the above-mentioned method. Considering the high proportion of shell outliers in this study, which was not related to cleaning methods, Sr ppm values, or specific environmental conditions, we would not recommend sampling bivalve shells for baseline determination in future projects. Noteworthy exceptions are the TIDO-TIBO-PULE and ALE-BAM-BAL site clusters, whose catchment areas are closely linked to the Tisza and the Danube floodplains. Recent results have shown that the aquifers of the river Tisza and the river Danube have an average $^{87}Sr/^{86}Sr$ ratio of 0.7096 (Palmer and Edmond, 1989; Price et al., 2004). The bivalve shell values of PULEM1, PULEM2, and TIBOM differed less than 0.0001 from that ratio and consequently fitted into the site-specific baseline range (0.70939–0.70983). Despite a slightly larger variation at ALE-BAL-BAM, the values of BAMM1, BAMM2, and ALEM differed from 0.0001 to almost 0.0004 from the river value and fitted into the site-specific baseline range (0.70927–0.71032).

4.2. From samples to scale-based baselines

The combination of baseline data from different sites was another way to improve the sample. However, the large variability of $^{87}Sr/^{86}Sr$ values within a specific geological unit (Fig. S34), and the overlap of these $^{87}Sr/^{86}Sr$ ratios between the distinct geological units (Fig. 5), support the hypothesis that the geological background is not a sufficient argument for combining baseline samples from different sites. The geographical proximity of the sites also can further not be considered as an argument, because different environmental settings within adjacent catchment areas can lead to distinct site-specific strontium isotope baseline ranges (see Fig. S6-S10, S19-S20, and S25-S32). Combining baseline samples without accounting for small-scale geographical heterogeneity can bias the determination of the site-specific baseline and result in a micro-regional baseline (see 4.2). Broad and homogeneous regions like the Southern Alföld can however be characterized by a very narrow strontium isotope baseline range despite a large geographical scale – though the sample size could be too small to be considered representative for the whole study area (Fig. S21-S22). The distance between the individual sites is consequently not a decisive criterion in the baseline composition. A clear 'cut-off' value between site-specific, (micro-)regional, and non-local remains difficult to establish, partly because of the fluid transitions and overlaps in geological and other environmental settings (Price et al., 2002; Vohberger, 2011). This study demonstrates the important role of multicriteria environmental analyses and the consideration of site-catchment areas in strontium isotope baseline determination.

Strontium isotope analyses often focus on a single site or a cluster of a few sites within a specific region. The determination of the baseline is consequently targeted to only interpret the data from the site or the site cluster (Gerling et al., 2012; Giblin et al., 2013; Knipper et al., 2018; Naumann et al., 2014). To determine a so-called 'local' baseline, two main approaches have been suggested. The first method consists of exclusively collecting samples from the site (Guede et al., 2018). The second integrates additional samples from the surroundings to the samples collected at the site (Alt et al., 2014; Hemer et al., 2014; Knipper et al., 2014, 2018; McManus et al., 2013; Wong et al., 2018). In this study, the first approach was applied because of restricted data availability. Published comparison data from the surroundings were only available for a few sites. The second approach, however, raises the question of the geographical location and the distance of the collected data compared to the site. A large variety of scale-based approaches to the extent of human activity ranges have been proposed in the context of isotope baseline determination. 'Local' ranges of 2 km (Knipper et al., 2012), 3 km (Kempf, 2020d), 12 km (Alt et al., 2014), 50 km (Brönnimann et al., 2018), 80 km (McManus et al., 2013), and even up to 180 km (Wong et al., 2018) proofed a high flexibility in the terminological discussions about scaled approaches in archaeology. In this study, the determination of local strontium isotope baseline was not only tied to distance-related buffers but rather to site-catchments with potential agricultural fields, pastures, and areas of constant human-environment interaction.

Confronting scales in archaeology is problematic – not only in terms of demographic estimations but also concerning site-catchment analysis or the determination of a local, site-specific, micro-regional, and macro-regional isotope baseline (Laabs and Knitter, 2021; Lock and Molyneaux, 2007; Müller and Diachenko, 2019; Roper, 1979; Volkmann, 2018). Even though the supra-regional understanding of ecological feedbacks and interconnections is inevitable for the interpretation of large-scale natural environmental networks (Brandolini and Carrer, 2020; Carrero-Pazos, 2019; Costanzo et al., 2021; Knitter et al., 2018; Laabs and Knitter, 2021), this study shows that an additional small-scale site-location analysis fosters the knowledge of the complex relationships between geological layers, pedological coverage, surface-cover development, and the hydrological system, which control the local human behavior and eventually the bioavailable isotopic composition of the local community's foodstuffs (Crowley et al., 2017; Kempf, in preparation, 2020d). On the other hand, applied to specific chronological or social entities, a cultural component should be considered in the analysis, since political, economic, and technological issues play an important role in the extent of the sphere of interaction and the process of food acquisition. Hence, the determination of a local strontium isotope baseline is a complex component in the evaluation of past mobile social systems that can be considered a constant adaptation to the environmental and cultural components coupled in the group's interaction sphere (Kempf, 2020b, 2020c; Knitter et al., 2018; Kolář et al., 2016; Kolář, 2020; Llobera, 1996, 2012). The processes behind the models, however, vary over space and time and the observations supporting the analyses are conditional to large-scale environmental and socio-cultural developments. Stationary data values have the potential to hide the dynamic processes behind the generation of the samples and thus to lead to a spatially local interpretation instead of a rather increased and supraregional human mobility.

Strontium isotope analyses in archaeological projects are usually led to investigate human or faunal mobility (Alt et al., 2014; Gerling et al., 2017; Hoekman-Sites and Giblin, 2012; Knipper et al., 2012, 2014, 2018). Defining baselines related to different scales nonetheless allows broadening the spectrum of possible interpretations, because site-outliers are not systematically a proof for long-distance migrations but may also originate from a nearby site. However, the identification of various patterns is inherently linked to the determination of the local baseline. There were already some attempts to estimate regional baseline ranges (Blank et al., 2018; Pacheco-Forés et al., 2020; Sjögren et al., 2016; Whelton et al., 2018), but defining various baseline ranges for investigating mobility patterns at one site is still a challenge (Knipper et al., 2014, 2018, 2020). In this study, the distinction between site-specific and micro-regional baseline ranges was enabled by the large number of studied sites, their geographical distribution, and the integration of small-scale multicriteria environmental analyses.

Applied to the study of past mobilities, this enables to identify mobility patterns within the surrounding area of the sites. This issue has been addressed by Claudia Gerling (Gerling, 2015), who suggested a regional strontium isotope baseline range for the Sárrét region

(0.709–0.711). The lack of data and the large extent of the research area did not enable the determination of each site's local baseline range (Gerling, 2015). However, compared to this regional range, each site from this area in our study shows a narrower site-specific baseline range (see Debrecen Tócópart Erdöalja (TOPE) and Ebes-Zsong-völgy (EBVÖ) in Fig. S31-S32). Without the distinction between site-specific and (micro-)regional baseline, site-outliers would be underestimated when interpreting human dental enamel $^{87}Sr/^{86}Sr$ ratios.

4.3. Strontium isomap of Hungary

Hungary does not show homogeneous isotopic baseline ranges (Fig. 6a). The different environmental settings and the mixed sample characteristics have significant impact on the site-specific and the micro-regional isotopic composition (Fig. S1-S32). The broad floodplains of the river Danube and particularly the southern part of the river Tisza show similar baseline ranges covering a large part of the Hungarian Plain. However, an interpolation of the data spectra is not possible because the Danube-Tisza interfluve (DTI) separates the two floodplains by an elevated sandy plateau that consists of abandoned paleochannels and intra-riverbed islands of the early Holocene anastomosing river systems. The geological, pedological, and hydrological conditions, the surface water permeability, and eventually the potential vegetation coverage differ significantly from the faunal and floral composition of the adjacent floodplains. Even though the rather plain landscape of the central and southern part of Hungary appears to be comparable in terms of similar isotopic data, the DTI shows not only less favorable land-use and settlement conditions but also no reliable data density to integrate the specific region into the hydrogeographical system of the rivers Danube and Tisza.

The DTI reveals only two sample sites (Cegléd: CGIP and CEG), which show different local isotopic baseline ranges within one shared micro-region (Fig. 6b, Table 2). The location at the eastern margins of the DTI is particularly visible in the baseline range of Cegléd (CEG) that rather fits to the river Tisza floodplain baseline range. The marginal location parameters illustrate the blurred transition from one region to another. None of the regional classifications shows sharp transitions but rather continuous transformation with mosaic geological and pedological units. Particularly, the fluvial surface characteristics of the small river systems draining the DTI produced an interchanging mixed sediment composition, which depends on flooding events, land-use, and the subsequent increase of erosion and sediment transport during extreme precipitation events. The stratified sedimentation regime forms a gradual change in soil texture from the north to the south. The sedimentological fractionation further influences the isotopic composition of the bioavailable strontium. The baseline ranges of the river Tisza floodplain (Fig. 6c) illustrate the gradient of the isotopic values depending on the sedimentological budget of the river Tisza and the tributaries draining the eastern Carpathian Mountain range, the Nyírség, and the Great Hungarian Range to the north. The baseline ranges of the western margins of the region Nyírség are comparable to the local baseline ranges of the eastern river Tisza floodplain region, which emphasizes the feedbacks of the strontium ratio values and the composition of the sediment load.

The same pattern can be detected in the southern floodplain of the river Danube and the eastern margins of the Transdanubian region (Fig. 6b). The sediment input of the west-east draining tributaries to the river Danube produced a mixed geological signal in the valleys and the foothill area of the western bank of the floodplain. The Alsónyék – Bátaszék and Mórágy – Tűzkődomb site cluster (BAM, BAL, ALE, and MORT) shows a mixed isotopic baseline range and a micro-regional range that is composed of the floodplain signal produced by fine-grained sediment layers, the aquifer of the river Danube, and the local geological signal of the Transdanubian Range (Fig. S13-S14) (Depaermentier et al., 2020b). The site cluster from the eastern Baranya County (BORK, M6-116, LGCS, VEGI, SEKU and SZEH) is situated to the south of the Alsónyék – Bátaszék – Mórágy cluster. The geological signals are very heterogeneous with loess coverage interchanging with mudstones and fluvial sediments (Fig. S15). The local and micro-regional baseline ranges, however, show a very narrow extent and a close relationship to the river Danube floodplain baselines (Fig. S16). This might be due to relocated silty material at the margins of the floodplain of the river Danube that has been deposited during Holocene flooding events and surface transformation. Due to the small-scale variability in environmental settings and strontium isotope composition, we consider the interpolation of site-specific baseline ranges on the isomap as inappropriate.

5. Conclusions

There is ongoing debate in archaeological research on the reliability isotope analyses and to which extent a strontium isotopic value can explain patterned behavior of individuals and groups in a specific landscape. One of the major limitations of the attempt to reconstruct potential palaeoenvironments and mobility and human-landscape interaction is the often limited number of statistically significant samples in supraregional and large-scale research areas and the unbalanced selection of sample material (Guede et al., 2018; McManus et al., 2013; Naumann et al., 2014). Archaeology is by itself limited to an impossible reconstruction of human behavior in specific parts of the landscape, however, the combination of a low number of archaeological sites and a low number of palaeoenvironmental samples risks inflating the expectations of a comprehensive socio-environmental explanation of human behavioral patterns. All too rapidly, new narratives of human evolution, technological developments, and large-scale migration processes are proposed that neither mirror the archaeological material nor the manifold ways how to interpret the results of the scientific analyses and particularly strontium isotope data. The determination of a reliable baseline depends on both the quantity and the quality of the baseline samples. However, for logistical, time, and financial reasons, it is not always possible to fulfil the established requirements (Bataille et al., 2020; Brönnimann et al., 2018; Makarewicz and Sealy, 2015).

In this paper, a new approach enabled to deal with challenging datasets for the determination of strontium isotope baselines in Hungary. A combination of multicriteria environmental modelling and strontium isotope analyses enabled highlighting significant small-scale geographical differences between 49 sites in Hungary. This combination allowed avoiding an extensive baseline range among inappropriate locations that show incomparable environmental settings – despite their adjacent location. Consequently, the Hungarian strontium isomap presented here emphasizes the site-specific and the micro-regional scale instead of interpolating an isoscape from point-based strontium data. The distinction between site-specific and micro-regional baselines allows for recognizing mobility patterns and subsistence strategies on different scales through the interpretation of human dental enamel $^{87}Sr/^{86}Sr$ ratios.

Authors contributions

Conceived and designed the experiments: MLCD, MK. Performed the experiments: MLCD, MK. Analysed the data: MLCD, MK. Wrote the paper: MLCD, MK, EB, KWA. Editing and revision: MLCD, MK. Cemeteries partially excavated: EB.

Declaration of competing interest

The authors declare no conflict of interest.

Acknowledgements

We would like to thank three anonymous reviewers for their constructive and critical suggestions, which have strengthened the

approach behind this article. We are very further grateful to Bethany Turner and Marcos Martinón-Torres for their advice during the revision process. This research was supported by the German Research Foundation (Al 287/10-1). We are particularly grateful to Corina Knipper and colleagues from the CEZA at Mannheim for their support during the final stage of the paper. We would also like to thank János Jakucs, Alexander Mörseburg, Anna Szécsényi-Nagy, Alexandra Anders, Piroska Csengeri, Róbert Patay, Katalin Sebők, Marc Fecher, Balázs G. Mende, and Kitti Köhler who provided insights and expertise, which greatly assisted the research. MK received funding from the Czech Republic under grant number CZ.02.2.69/0.0/0./18_053/0016952; Postdoc2MUNIm order number 21 0053; Masaryk University, Brno, Czech Republic.

Appendix A. Supplementary data

Supplementary data to this article can be found online at https://doi.org/10.1016/j.jas.2021.105489.

References

Ács, F., Breuer, H., Skarbit, N., 2015. Climate of Hungary in the twentieth century according to Feddema. Theor. Appl. Climatol. 119 (1–2), 161–169. https://doi.org/10.1007/s00704-014-1103-5.

Alonzi, E., et al., 2020. New understandings of the sea spray effect and its impact on bioavailable radiogenic strontium isotope ratios in coastal environments. J. Archaeol. Sci.: Report 33, 102462. https://doi.org/10.1016/j.jasrep.2020.102462.

Alt, K.W., et al., 2014. 'Lombards on the move – an integrative study of the migration period cemetery at szólád, Hungary'. PloS One 9 (11). https://doi.org/10.1371/journal.pone.0110793.

Balasse, M., et al., 2002. The seasonal mobility model for prehistoric herders in the south-western cape of South Africa assessed by isotopic analysis of sheep tooth enamel. J. Archaeol. Sci. 29 (9), 917–932. https://doi.org/10.1006/jasc.2001.0787.

Bánffy, E., 2013. *The Early Neolithic in the Danube-Tisza Interfluve.* (Archaeolingua Central European Series, 7). Archaeopress, Oxford.

Bartelink, E.J., Chesson, L.A., 2019. Recent applications of isotope analysis to forensic anthropology. Forensic Sciences Research 4 (1), 29–44. https://doi.org/10.1080/20961790.2018.1549527.

Bataille, C.P., et al., 2020. Advances in global bioavailable strontium isoscapes. Palaeogeogr. Palaeoclimatol. Palaeoecol. 555, 109849. https://doi.org/10.1016/j.palaeo.2020.109849.

Bataille, C.P., Bowen, G.J., 2012. Mapping 87Sr/86Sr variations in bedrock and water for large scale provenance studies. Chem. Geol. 304–305, 39–52. https://doi.org/10.1016/j.chemgeo.2012.01.028.

Bentley, R.A., 2006. Strontium isotopes from the earth to the archaeological skeleton: a review. J. Archaeol. Method Theor 13 (3), 135–187. https://doi.org/10.1007/s10816-006-9009-x.

Bentley, R.A., Price, T.D., Stephan, E., 2004. 'Determining the 'local' 87Sr/86Sr range for archaeological skeletons: a case study from Neolithic Europe'. J. Archaeol. Sci. 31 (4), 365–375. https://doi.org/10.1016/j.jas.2003.09.003.

Birkás, M., et al., 2004. Tillage effects on compaction, earthworms and other soil quality indicators in Hungary. Soil Tillage Res. 78 (2), 185–196. https://doi.org/10.1016/j.still.2004.02.006.

Blank, M., et al., 2018. Isotope values of the bioavailable strontium in inland southwestern Sweden-A baseline for mobility studies. PloS One 13 (10), e0204649. https://doi.org/10.1371/journal.pone.0204649.

Bozán, C., et al., 2018. Integrated spatial assessment of inland excess water hazard on the Great Hungarian Plain. Land Degrad. Dev. 29 (12), 4373–4386. https://doi.org/10.1002/ldr.3187.

Brandolini, F., Carrer, F., 2020. Terra, Silva et Paludes. Assessing the Role of Alluvial Geomorphology for Late-Holocene Settlement Strategies (Po Plain – N Italy) Through Point Pattern Analysis. Environ. Archaeol. 1–15. https://doi.org/10.1080/14614103.2020.1740866.

Brettell, R., et al., 2012. ''Impious easterners': can oxygen and strontium isotopes serve as indicators of provenance in early medieval European cemetery populations? Eur. J. Archaeol. 15 (1), 117–145. https://doi.org/10.1179/1461957112Y.0000000001.

Brönnimann, D., et al., 2018. The lay of land: strontium isotope variability in the dietary catchment of the Late Iron Age proto-urban settlement of Basel-Gasfabrik, Switzerland. J. Archaeol. Sci.: Report 17, 279–292. https://doi.org/10.1016/j.jasrep.2017.11.009.

Carlson, D.L., 2017. *Quantitative Methods in Archaeology Using R.* (Cambridge Manuals in Archaeology). Cambridge University Press, Cambridge.

Carrero-Pazos, M., 2019. Density, intensity and clustering patterns in the spatial distribution of Galician megaliths (NW Iberian Peninsula). Archaeological and Anthropological Sciences 11 (5), 2097–2108. https://doi.org/10.1007/s12520-018-0662-2.

Corti, C., et al., 2013. On the use of trace elements in ancient necropolis studies: overview and ICP-MS application to the case study of Valdaro site. Italy', *Microchemical Journal* 110, 614–623. https://doi.org/10.1016/j.microc.2013.07.001.

Costanzo, S., et al., 2021. Creating the funerary landscape of Eastern Sudan. PloS One 16 (7), e0253511. https://doi.org/10.1371/journal.pone.0253511.

Crowley, B.E., Miller, J.H., Bataille, C.P., 2017. Strontium isotopes (87 Sr/86 Sr) in terrestrial ecological and palaeoecological research: empirical efforts and recent advances in continental-scale models. Biol. Rev. Camb. Phil. Soc. 92 (1), 43–59. https://doi.org/10.1111/brv.12217.

Demény, A., et al., 2013. Mid-Holocene climate conditions and moisture source variations based on stable H, C and O isotope compositions of speleothems in Hungary. Quat. Int. 293, 150–156. Accessed: (Accessed 26 August 2019).

Depaermentier, M.L.C., et al., 2020a. 'Neolithic land-use, subsistence, and mobility patterns in Transdanubia: a multiproxy isotope and environmental analysis from Alsónyék – Bátaszék and Mórágy – Tűzkődomb'. J. Archaeol. Sci.: Report 33 (17pp). https://doi.org/10.1016/j.jasrep.2020.102529.

Depaermentier, M.L.C., et al., 2020b. Tracing mobility patterns through the 6th-5th millennia BC in the Carpathian Basin with strontium and oxygen stable isotope analyses. PloS One. https://doi.org/10.1371/journal.pone.0242745.

EGDI, 2020. *Hydrogeological Map Of Europe (IHME 1500)*: Geological Survey Organisations of Europe.

Evans, J.A., et al., 2010. Spatial variations in biosphere 87 Sr/86 Sr in Britain. J. Geol. Soc. 167 (1), 1–4. https://doi.org/10.1144/0016-76492009-090.

Fitzsimmons, K.E., Marković, S.B., Hambach, U., 2012. Pleistocene environmental dynamics recorded in the loess of the middle and lower Danube basin. Quat. Sci. Rev. 41, 104–118. https://doi.org/10.1016/j.quascirev.2012.03.002.

Frei, R., Frei, K.M., Jessen, S., 2020. Shallow retardation of the strontium isotope signal of agricultural liming - implications for isoscapes used in provenance studies. Sci. Total Environ. 706, 135710. https://doi.org/10.1016/j.scitotenv.2019.135710.

García-Suárez, A., Portillo, M., Matthews, W., 2020. Early animal management strategies during the neolithic of the konya plain, central anatolia: integrating micromorphological and microfossil evidence. Environ. Archaeol. 25 (2), 208–226. https://doi.org/10.1080/14614103.2018.1497831.

Gerling, C., et al., 2012. Immigration and transhumance in the early bronze age Carpathian Basin: the occupants of a kurgan. Antiquity 86 (334), 1097–1111. https://doi.org/10.1017/S0003598X00048274.

Gerling, C., 2015. Prehistoric Mobility and Diet in the West Eurasian Steppes 3500 to 300 BC: an Isotopic Approach, vol. 25. De Gruyter, Berlin.

Gerling, C., et al., 2017. High-resolution isotopic evidence of specialised cattle herding in the European Neolithic. PloS One 12 (7), e0180164. https://doi.org/10.1371/journal.pone.0180164.

Giblin, J.I., 2009. Strontium isotope analysis of neolithic and copper age populations on the Great Hungarian plain. J. Archaeol. Sci. 36 (2), 491–497. https://doi.org/10.1016/j.jas.2008.09.034.

Giblin, J.I., et al., 2013. Strontium isotope analysis and human mobility during the Neolithic and Copper Age: a case study from the Great Hungarian Plain. J. Archaeol. Sci. 40 (1), 227–239. https://doi.org/10.1016/j.jas.2012.08.024.

Grupe, G., et al., 1997. Mobility of Bell Beaker people revealed by strontium isotope ratios of tooth and bone: a study of southern Bavarian skeletal remains. Appl. Geochem. 12 (4), 517–525. https://doi.org/10.1016/S0883-2927(97)00030-9.

Guede, I., et al., 2018. Isotopic evidence for the reconstruction of diet and mobility during village formation in the Early Middle Ages: las Gobas (Burgos, northern Spain). Archaeological and Anthropological Sciences 10 (8), 2047–2058. Accessed: (Accessed 30 October 2019).

Haynes, W., 2013. 'Tukey's test'. In: Dubitzky, W., et al. (Eds.), Encyclopedia of Systems Biology. Springer New York, New York, NY, pp. 2303–2304.

Heinrich-Tamáska, O., Schweissing, M., 2011. Strontiumisotopen- und Radiokarbonuntersuchungen am anthropologischen Fundmaterial von Keszthle-Fenékpuszta: ihr Aussagepotential zur Fragen der Migration und Chronologie. In: Heinrich-Tamáska, O. (Ed.), *Keszthely-Fenékpuszta im Kontext spätantiker Kontinuitätsforschung zwischen Noricum und Moesia.* (Castellum Pannonicum Pelsonense, 2). Rahden/Westf., Leidorf, pp. 457–474.

Hemer, K.A., et al., 2014. No Man is an island: evidence of pre-Viking Age migration to the Isle of Man. J. Archaeol. Sci. 52, 242–249. https://doi.org/10.1016/j.jas.2014.08.031.

Hoekman-Sites, H.A., Giblin, J.I., 2012. Prehistoric animal use on the Great Hungarian Plain: a synthesis of isotope and residue analyses from the Neolithic and Copper Age. J. Anthropol. Archaeol. 31 (4), 515–527. https://doi.org/10.1016/j.jaa.2012.05.002.

Hoogewerff, J.A., et al., 2019. Bioavailable 87Sr/86Sr in European soils: a baseline for provenancing studies. Sci. Total Environ. 672, 1033–1044. https://doi.org/10.1016/j.scitotenv.2019.03.387.

Howey, M.C.L., 2011. Multiple pathways across past landscapes: circuit theory as a complementary geospatial method to least cost path for modeling past movement. J. Archaeol. Sci. 38 (10), 2523–2535. https://doi.org/10.1016/j.jas.2011.03.024.

Kempf, M. (in preparation) 'Take a Seed! Revealing Neolithic Landscape and Agricultural Development in the Carpathian Basin through Multivariate Statistics and Environmental Modelling'.

Kempf, M., 2019. Paradigm and pragmatism: GIS-based spatial analyses of Roman infrastructure networks and land-use concepts in the Upper Rhine Valley. Geoarchaeology 74 (285), 1–12. https://doi.org/10.1002/gea.21752.

Kempf, M., 2020a. Fables of the past: landscape (re-)constructions and the bias in the data. Documenta Praehistorica 47, 476–492. https://doi.org/10.4312/dp.47.27.

Kempf, M., 2020b. From landscape affordances to landscape connectivity: contextualizing an archaeology of human ecology. Archaeological and Anthropological Sciences 12 (8), 310. https://doi.org/10.1007/s12520-020-01157-4.

Kempf, M., 2020c. Modeling multivariate landscape affordances and functional ecosystem connectivity in landscape archeology. Archaeological and

Anthropological Sciences 12 (8), 1–21. https://doi.org/10.1007/s12520-020-01127-w.
Kempf, M., 2020d. Neolithic land-use, landscape development, and environmental dynamics in the Carpathian Basin. J. Archaeol. Sci.: Report 34, 102637. https://doi.org/10.1016/j.jasrep.2020.102637.
Kercsmár, Z., et al., 2015. In: Surface Geology of Hungary: Explanatory Notes to the Geological Map of Hungary (1:500 000). Geological and Geophysical Institute of Hungary, Budapest.
Kiss, T., et al., 2015. 'The evolution of the Great Hungarian Plain fluvial system – fluvial processes in a subsiding area from the beginning of the Weichselian'. Quat. Int. 388, 142–155. https://doi.org/10.1016/j.quaint.2014.05.050.
Knipper, C., 2004. Die Strontiumisotopenanalyse: eine naturwissenschaftliche Methode zur Erfassung von Mobilität in der Ur- und Frühgeschichte. Jahrbuch des Römisch-Germanischen Zentralmuseums (51), 589–685. https://doi.org/10.11588/JRGZM.2004.2.21081.
Knipper, C., et al., 2012. Mobility in Thuringia or mobile Thuringians: a strontium isotope study from early medieval Central Germany. In: Schier, W., Kaiser, E., Burger, J. (Eds.), *Population Dynamics In Prehistory And Early History. New Approaches Using Stable Isotopes And Genetics.* s.L. De Gruyter.
Knipper, C., et al., 2014. 'Social differentiation and land use at an Early Iron Age "princely seat": bioarchaeological investigations at the Glauberg (Germany)'. J. Archaeol. Sci. 41, 818–835. https://doi.org/10.1016/j.jas.2013.09.019.
Knipper, C., 2017. Sampling for stable isotope analyses in archaeology. Information potential, strategies, and documentation. In: Molodin, V., Hansen, S. (Eds.), Multidisciplinarnye Metody V Archeologii Novejšie Itogi I Perspektivy: Materialy Meždunarodnogo Simpoziuma "Multidisciplinarnye Metody V Archeologii: Novejšie Itogi I Perspektivy, pp. 84–94 (22-26 ijunja 2015 g. g. Novosibirsk). Novosibirsk.
Knipper, C., et al., 2018. A knot in a network: residential mobility at the Late Iron Age proto-urban centre of Basel-Gasfabrik (Switzerland) revealed by isotope analyses. J. Archaeol. Sci.: Report 17, 735–753. https://doi.org/10.1016/j.jasrep.2017.12.001.
Knipper, C., et al., 2020. Coalescing traditions-coalescing people: community formation in pannonia after the decline of the roman empire. PloS One 15 (4). https://doi.org/10.1371/journal.pone.0231760.
Knitter, D., et al., 2018. Critical physical geography in practice: landscape archaeology. In: Lave, R., Biermann, C., Lane, S.N. (Eds.), *The Palgrave Handbook of Critical Physical Geography.* (Palgrave Handbooks). Palgrave Macmillan, Cham, pp. 179–200. Accessed: (Accessed 8 December 2019).
Knudson, K.J., et al., 2012. Migration and Viking Dublin: paleomobility and paleodiet through isotopic analyses. J. Archaeol. Sci. 39 (2), 308–320. https://doi.org/10.1016/j.jas.2011.09.014.
Knudson, K.J., et al., 2014. Baseline data for Andean paleomobility research: a radiogenic strontium isotope study of modern Peruvian agricultural soils. Archaeological and Anthropological Sciences 6 (3), 205–219. https://doi.org/10.1007/s12520-013-0148-1.
Koehler, G., Kardynal, K.J., Hobson, K.A., 2019. Geographical assignment of polar bears using multi-element isoscapes. Sci. Rep. 9 (1), 9390. https://doi.org/10.1038/s41598-019-45874-w.
Kolář, J., et al., 2016. Spatio-temporal modelling as a way to reconstruct patterns of past human activities. Archaeometry 58 (3), 513–528. https://doi.org/10.1111/arcm.12182.
Kolář, J., 2020. Migrations or local interactions? Spheres of interaction in third-millennium BC Central Europe. Antiquity 94 (377), 1168–1185. https://doi.org/10.15184/aqy.2020.151.
Kulp, J.L., Turekian, K.K., 1956. Strontium content of human bones. Science 124 (3218), 405–407. https://doi.org/10.1126/science.124.3218.405-a.
Laabs, J., Knitter, D., 2021. How much is enough? First steps to a social ecology of the pergamon microregion. Land 10 (5), 479. https://doi.org/10.3390/land10050479.
Laborczi, A., et al., 2016. Mapping of topsoil texture in Hungary using classification trees. J. Maps 12 (5), 999–1009. https://doi.org/10.1080/17445647.2015.1113896.
Laborczi, A., et al., 2019. Comparison of soil texture maps synthetized from standard depth layers with directly compiled products. Geoderma 352, 360–372. https://doi.org/10.1016/j.geoderma.2018.01.020.
Ladegaard-Pedersen, P., et al., 2020. A strontium isotope baseline of Cyprus. Assessing the use of soil leachates, plants, groundwater and surface water as proxies for the local range of bioavailable strontium isotope composition. Sci. Total Environ. 708, 134714. https://doi.org/10.1016/j.scitotenv.2019.134714.
Llobera, M., 1996. Exploring the topography of mind: GIS, social space and archaeology. Antiquity 70 (269), 612–622. https://doi.org/10.1017/S0003598X00083745.
Llobera, M., 2012. 'Life on a pixel: challenges in the development of digital methods within an "interpretive" landscape archaeology framework'. J. Archaeol. Method Theor 19 (4), 495–509. https://doi.org/10.1007/s10816-012-9139-2.
Lock, G.R., Molyneaux, B., 2007. Confronting Scale in Archaeology: Issues of Theory and Practice. Springer, New York.
Longman, J., et al., 2019. Runoff events and related rainfall variability in the Southern Carpathians during the last 2000 years. Sci. Rep. 9 (1), 5334. https://doi.org/10.1038/s41598-019-41855-1.
Makarewicz, C.A., Sealy, J., 2015. Dietary reconstruction, mobility, and the analysis of ancient skeletal tissues: expanding the prospects of stable isotope research in archaeology. J. Archaeol. Sci. 56, 146–158. https://doi.org/10.1016/j.jas.2015.02.035.
Maurer, A.-F., et al., 2012. Bioavailable 87Sr/86Sr in different environmental samples - effects of anthropogenic contamination and implications for isoscapes in past migration studies. Sci. Total Environ. 433, 216–229. https://doi.org/10.1016/j.scitotenv.2012.06.046.
McManus, E., et al., 2013. '"To the land or to the sea": diet and mobility in early medieval frisia'. J. I. Coast Archaeol. 8 (2), 255–277. https://doi.org/10.1080/15564894.2013.787565.
Montgomery, J., 2010. Passports from the past: investigating human dispersals using strontium isotope analysis of tooth enamel. Ann. Hum. Biol. 37 (3), 325–346. https://doi.org/10.3109/03014461003649297.
Müller, J., Diachenko, A., 2019. Tracing long-term demographic changes: the issue of spatial scales. PloS One 14 (1), e0208739. https://doi.org/10.1371/journal.pone.0208739.
Müller-Sohnius, D., 2007. 87Sr/86Sr for Isotope Standards of Eimer and Amend (E&A), Modern Seawater Strontium (MSS), and the Standard Reference Material (SRM) 987: Development of Interlaboratory Mean Values, Procedures of Adjusting, and the Comparability of Results. Geologica Bavarica, pp. 1–56, 110.
Munro, N.D., Stiner, M.C., 2020. A zooarchaeological history of the Neolithic occupations at Franchthi Cave and paralia in southern Greece. J. Anthropol. Archaeol. 58, 101162. https://doi.org/10.1016/j.jaa.2020.101162.
Nakoinz, O., Knitter, D., 2016. *Modelling Human Behaviour in Landscapes: Basic Concepts and Modelling Elements*. (Quantitative Archaeology and Archaeological Modelling). Springer International Publishing, Cham.
National Institute of Standards & Technology, 2007. Certificate of Analysis Standard Reference Material 987 (Gaithersburg).
Naumann, E., Price, T.D., Richards, M.P., 2014. Changes in dietary practices and social organization during the pivotal late iron age period in Norway (AD 550-1030): isotope analyses of Merovingian and Viking Age human remains. Am. J. Phys. Anthropol. 155 (3), 322–331. https://doi.org/10.1002/ajpa.22551.
Négyesi, G., et al., 2019. Wind erosion researches in Hungary – past, present and future possibilities. Hungarian Geographical Bulletin 223–240. https://doi.org/10.15201/hungeobull.68.3.2.
Nelson, B.K., et al., 1986. Effects of diagenesis on strontium, carbon, nitrogen and oxygen concentration and isotopic composition of bone. Geochem. Cosmochim. Acta 50 (9), 1941–1949. https://doi.org/10.1016/0016-7037(86)90250-4.
Obreht, I., et al., 2019. A critical reevaluation of palaeoclimate proxy records from loess in the Carpathian Basin. Earth Sci. Rev. 190, 498–520. https://doi.org/10.1016/j.earscirev.2019.01.020.
Oelze, V.M., Nehlich, O., Richards, M.P., 2012. 'There's no place like home' - no isotopic evidence for mobility at the Early Bronze Age cemetery of Singen. Germany', *Archaeometry* 54 (4), 752–778. https://doi.org/10.1111/j.1475-4754.2011.00644.x.
Pacheco-Forés, S.I., Gordon, G.W., Knudson, K.J., 2020. Expanding radiogenic strontium isotope baseline data for central Mexican paleomobility studies. PloS One 15 (2), e0229687. https://doi.org/10.1371/journal.pone.0229687.
Palmer, M.R., Edmond, J.M., 1989. The strontium isotope budget of the modern ocean. Earth Planet Sci. Lett. 92 (1), 11–26. https://doi.org/10.1016/0012-821X(89)90017-4.
Pásztor, L., et al., 2012. Compilation of 1:50,000 scale digital soil maps for Hungary based on the digital Kreybig soil information system. J. Maps 8 (3), 215–219. https://doi.org/10.1080/17445647.2012.705517.
Pásztor, L., et al., 2015a. Compilation of novel and renewed, goal oriented digital soil maps using geostatistical and data mining tools. Hungarian Geographical Bulletin 64 (1), 49–64. https://doi.org/10.15201/hungeobull.64.1.5.
Pásztor, L., et al., 2015b. Spatial risk assessment of hydrological extremities: inland excess water hazard, Szabolcs-Szatmár-Bereg County, Hungary. J. Maps 11 (4), 636–644. https://doi.org/10.1080/17445647.2014.954647.
Pásztor, L., et al., 2018. Compilation of a national soil-type map for Hungary by sequential classification methods. Geoderma 311, 93–108. https://doi.org/10.1016/j.geoderma.2017.04.018.
Price, D.T., et al., 2012. Isotopes and mobility. Case studies with large samples. In: Kaiser, E., Burger, J., Schier, W. (Eds.), Population Dynamics in Prehistory and Early History: New Approaches by Using Stable Isotopes and Genetic. De Gruyter, Berlin, Boston, pp. 311–321.
Price, T.D., et al., 2004. Strontium isotopes and prehistoric human migration: the bell beaker period in central europe. Eur. J. Archaeol. 7 (1), 9–40. https://doi.org/10.1177/1461957104047992.
Price, T.D., Burton, J.H., Bentley, R.A., 2002. The characterization of biologically available strontium isotope ratios for the study of prehistoric migration. Archaeometry 44 (1), 117–135. Accessed: 20 September 2019).
Price, T.D., Manzanilla, L., Middleton, W.D., 2000. Immigration and the ancient city of teotihuacan in Mexico: a study using strontium isotope ratios in human bone and teeth. J. Archaeol. Sci. 27 (10), 903–913. https://doi.org/10.1006/jasc.1999.0504.
R Core Team and contributors worldwide, 2021. The R Stats Package. R Core Team. Available at:, Version 4.2.0. https://stat.ethz.ch/R-manual/R-devel/library/stats/html/00Index.html.
Roper, D.C., 1979. The method and theory of site catchment analysis: a review. Adv. Archaeol. Method Theor. 2, 119–140. Accessed: (Accessed 6 November 2019).
Scheu, A., 2018. Neolithic animal domestication as seen from ancient DNA. Quat. Int. 496, 102–107. https://doi.org/10.1016/j.quaint.2017.02.009.
Schweissing, M.M., Grupe, G., 2003. Stable strontium isotopes in human teeth and bone: a key to migration events of the late Roman period in Bavaria. J. Archaeol. Sci. 30 (11), 1373–1383. https://doi.org/10.1016/S0305-4403(03)00025-6.
Shaw, B.J., et al., 2009. The use of strontium isotopes as an indicator of migration in human and pig Lapita populations in the Bismarck Archipelago, Papua New Guinea. J. Archaeol. Sci. 36 (4), 1079–1091. https://doi.org/10.1016/j.jas.2008.12.010.
Sherratt, A., 1983. The development of neolithic and copper age settlement in the Great Hungarian plain: Part II: site survey and settlement dynamics. Oxf. J. Archaeol. 2 (1), 13–41. Accessed: (Accessed 6 November 2019).
Sjögren, K.-G., Price, T.D., Kristiansen, K., 2016. Diet and mobility in the corded ware of central europe. PloS One 11 (5). https://doi.org/10.1371/journal.pone.0155083.

Slovak, N.M., Paytan, A., 2011. Applications of Sr isotopes in archaeology. In: Baskaran, M. (Ed.), *Handbook Of Environmental Isotope Geochemistry.* (Advances in Isotope Geochemistry). Springer, Heidelberg, pp. 743–768.

Snoeck, C., et al., 2020. Towards a biologically available strontium isotope baseline for Ireland. Sci. Total Environ. 712, 136248. https://doi.org/10.1016/j.scitotenv.2019.136248.

Stiner, M.C., et al., 2014. A forager-herder trade-off, from broad-spectrum hunting to sheep management at Aşıklı Höyük, Turkey. Proc. Natl. Acad. Sci. U. S. A 111 (23), 8404–8409. https://doi.org/10.1073/pnas.1322723111.

Sümegi, P., Gulyas, S., Persaits, G., 2013. The geoarchaeological evolution of the loess-covered alluvial island of polgár and its role in shaping human settlement strategies. In: Anders, A., Kulcsár, G. (Eds.), *Moments In Time: Papers Presented to Pál Raczky On His 60th Birthday.* (Prehistoric Studies = Őrségészeti Tanulmányok, 1). L'Harmattan, Budapest, pp. 901–912.

Sümegi, P., Kertész, R., 2001. Palaeogeographic characteristic of the Carpathian Basin: an ecological trap during the early neolithic? In: Kertész, R., Makkay, J. (Eds.), From the Mesolithic to the Neolithic: Proceedings of the International Archaeological Conference Held in the Damjanich Museum of Szolnok, September 22 - 27, 1996. Archaeolingua Alapítvány, Budapest, pp. 405–416 (Archaeolingua, 11).

Tapody, R.O., et al., 2018. Radiocarbon-dated peat development: anthropogenic and climatic signals in a Holocene raised bog and lake profile from the Eastern part of the Carpathian Basin. Radiocarbon 60 (4), 1215–1226. https://doi.org/10.1017/RDC.2018.38.

Trickett, M.A., et al., 2003. An assessment of solubility profiling as a decontamination procedure for the 87Sr/86Sr analysis of archaeological human skeletal tissue. Appl. Geochem. 18 (5), 653–658. https://doi.org/10.1016/S0883-2927(02)00181-6.

Trueman, C.N., 2004. Forensic geology of bone mineral: geochemical tracers for post-mortem movement of bone remains. Geological Society, London, Special Publications 232 (1), 249–256. https://doi.org/10.1144/GSL.SP.2004.232.01.22.

Trueman, C.N., Tuross, N., 2002. Trace elements in recent and fossil bone apatite. Rev. Mineral. Geochem. 48 (1), 489–521. https://doi.org/10.2138/rmg.2002.48.13.

Trueman, C.N.G., et al., 2004. Mineralogical and compositional changes in bones exposed on soil surfaces in Amboseli National Park, Kenya: diagenetic mechanisms and the role of sediment pore fluids. J. Archaeol. Sci. 31 (6), 721–739. https://doi.org/10.1016/j.jas.2003.11.003.

Tucker, C.J., 1979. Red and photographic infrared linear combinations for monitoring vegetation. Rem. Sens. Environ. 8 (2), 127–150. https://doi.org/10.1016/0034-4257(79)90013-0.

Tukey, J.W., 1977. Exploratory Data Analysis. Addison-Wesley Pub, Reading, Mass.

Vaiglova, P., et al., 2018. Of cattle and feasts: multi-isotope investigation of animal husbandry and communal feasting at Neolithic Makriyalos, northern Greece. PloS One 13 (6), e0194474. https://doi.org/10.1371/journal.pone.0194474.

Várallay, G., 1989. Soil degradation processes and their control in Hungary. Land Degrad. Rehabil. 1, 171–188. Accessed: (Accessed 28 August 2019).

Vohberger, M., 2011. Lokal oder Eingewandert? Interpretationsmöglichkeiten und Grenzen lokaler Strontium- und Sauerstoffisotopensignaturen am Beispiel einer Altgrabung in Wenigumstadt. München. PhD thesis.

Volkmann, A., 2018. Methods and perspectives of geoarchaelogical site catchment analysis: identification of palaeoclimate indicators in the oder region from the iron to middle ages. In: Siart, C., Forbriger, M., Bubenzer, O. (Eds.), *Digital Geoarchaeology: New Techniques for Interdisciplinary Human-Environmental Research.* (Natural Science in Archaeology). Springer, Cham, Switzerland, pp. 27–44. Accessed: (Accessed 6 November 2019).

Whelton, H.L., et al., 2018. Strontium isotope evidence for human mobility in the Neolithic of northern Greece. J. Archaeol. Sci.: Report 20, 768–774. https://doi.org/10.1016/j.jasrep.2018.06.020.

Whittle, A., et al., 2013. Hungary. In: Bickle, P., Whittle, A. (Eds.), *The First Farmers of Central Europe: Diversity In LBK Lifeways.* (Cardiff Studies in Archaeology). Oxbow Books and the David Brown Book Company, Oakville, CT, pp. 49–100.

Wickham, H., 2016. *ggplot2: Elegant Graphics for Data Analysis*. (Use R!). Springer, Cham. https://doi.org/10.1007/978-3-319-24277-4. Available at:

Wong, W.W., et al., 2018. Stable isotopes of nitrate reveal different nitrogen processing mechanisms in streams across a land use gradient during wet and dry periods. Biogeosciences 15 (13), 3953–3965. https://doi.org/10.5194/bg-15-3953-2018.